UNIVERSITÀ di VERONA | Department of ECONOMICS

Working Paper Series
Department of Economics
University of Verona

Deep Quadratic Hedging

Alessandro Gnoatto, Silvia Lavagnini, Athena Picarelli

WP Number: 11 December 2022

ISSN: 2036-2919 (paper), 2036-4679 (online)

Deep Quadratic Hedging

Alessandro Gnoatto[1], Silvia Lavagnini[2], and Athena Picarelli[1]

[1]Department of Economics, University of Verona, 37129 Verona, Italy
[2]Department of Data Science and Analytics, BI Norwegian Business School, 0848 Oslo, Norway

December 24, 2022

Abstract

We present a novel computational approach for quadratic hedging in a high-dimensional incomplete market. This covers both mean-variance hedging and local risk minimization. In the first case, the solution is linked to a system of BSDEs, one of which being a backward stochastic Riccati equation (BSRE); in the second case, the solution is related to the Föllmer-Schweizer decomposition and is also linked to a BSDE. We apply (recursively) a deep neural network-based BSDE solver. Thanks to these approach, we solve high-dimensional quadratic hedging problems, providing the entire hedging strategies paths, which, in alternative, would require to solve high dimensional PDEs. We test our approach with a classical Heston model and with a multi-dimensional generalization of it. Due to the unboundedness of the variance process, existence and uniqueness results for the BSRE must be considered.

Keywords Deep hedging; Deep BSDE solver; Mean-variance hedging; Local risk minimization; Multidimensional Heston model.

1 Introduction

The problem of hedging a contingent claim is typically faced by a financial institution who sold a derivative to a customer and is hence confronted with a future liability, in the form of a positive random variable H representing the payoff at final time. Hedging of contingent claims is a central problem in financial mathematics. Due to the link between trading strategies of the hedger and stochastic integrals [20], this corresponds to the question whether the random variable H can be written in the form of a stochastic integral of the trading strategy with respect to a semimartingale. When such a representation holds for any possible choice of the contingent claim H, the market is said to be complete. The standard example in this case is given by the Black-Scholes [3] market model.

Completeness, however, is a property which is easily lost as soon as we consider even slight generalizations of the Black-Scholes market, e.g. by considering random coefficients due to stochastic volatility/stochastic interest rates, or if we allow for discontinuous price paths in the underlying security. This fact has motivated, in the last decades, the introduction of a multitude of alternative approaches to hedging in incomplete markets.

In this paper, we consider quadratic hedging in a pure diffusive setting, both in the form of mean-variance hedging, introduced in [4], [11], [34], and local risk minimization, proposed in [16], [15], [33] and [34]. For a survey of the two approaches, featuring also a complete list of early references, we refer to [35]. In the last decades, the two approaches have been studied by

several authors and extended in different directions: for stochastic volatility models, which are the focus of the present paper, we mention [24] concentrating on local risk minimization,[10] and [2] who discuss mean-variance hedging. For the class of affine stochastic volatility models, we refer to [7] and [27]. For recent results on mean-variance hedging we also refer to [8].

For mean-variance hedging, approaches based on the theory of stochastic optimal control are treated in [30] and [26]. We anticipate that the link with stochastic control theory will be very important in our approach as we shall see in the sequel.

Concerning the computation of quadratic hedging strategies we mention [21] and [22]: in these works the two approaches are compared in the context of certain stochastic volatility models. Both local risk minimization and mean-variance hedging are studied from a numerical point of view: the two methods are implemented in a Markovian framework by using PDE techniques in the form of the finite difference method. It is well known that such numerical methods for PDEs suffer from the curse of dimensionality, hence it seems difficult to apply quadratic hedging to contingent claims that depend on a high number of risk factors. This is the problem we would like to address in the present paper: namely, we would like to propose a computational strategy which makes the implementation of quadratic hedging feasible even when the number of underlying risk factors is large.

Our strategy is based on two observations. First of all, both quadratic hedging approaches can be treated from the point of view of backward stochastic differential equations (BSDEs). This link is particularly evident for mean-variance hedging, due to the very formulation of the problem as a stochastic control problem of linear quadratic type: the solution involves a system of two BSDEs that need to be solved sequentially. For local risk minimization, the link with BSDEs is not immediately clear in the original definition of local risk minimizing strategy. However, it is well known that finding local risk minimizing strategies is equivalent to finding the so-called Föllmer-Schweizer decomposition of the discounted payoff, which in turn involves the solution of a linear BSDE. In summary, both local risk minimization and mean-variance hedging can be treated from the point of view of BSDEs.

The second observation is the fact that high-dimensional BSDEs (or equivalently the associated PDEs via the Feynman-Kac formula) can be efficiently solved by means of deep learning methods. In recent years, the introduction of advanced and highly parallelized hardware, in particular graphic processing units, have motivated, among other factors, an increasing relevance of statistical learning methods for the solution of high-dimensional problems. In the context of the numerical methods for PDEs an already large stream of literature involves the numerical solution of high-dimensional PDEs by means of deep learning methods, where different quantities related to the solution function are approximated by deep artificial neural networks (ANNs).

Of particular relevance for our work are [12] and [19]. In these works, the starting point is to consider the BSDE associated to a particular PDE. The solution of the BSDE is then viewed as the minimizer of a stochastic control process involving a quadratic loss. Once the BSDE is discretized forward in time via a standard Euler scheme, the initial condition and the controls of the BSDE, at each point in time, are parametrized by a family of ANNs. The parameters of the ANNs are optimized by minimizing the expected squared distance between the known terminal condition and the terminal value of the discretized BSDE.

In view of the two observations above our approach consists in expressing both quadratic hedging approaches by means of the associated BSDEs and then apply the deep BSDE solver of [12] to solve for all quantities of interest in a diffusive setting of arbitrary dimension.

As a running example we consider a multi-asset and multi-factor version of the Heston model [23]. One the one side, such choice allows us, in the one-dimensional setting, to validate our numerical procedure against well established numerical solutions that employ standard

numerical methods, notably the results of [7]; on the other side, this hints at the possibility of applying our approach in the more broad class of diffusive stochastic volatility models. Our numerical results show that deep learning based methods increase the scope of applicability of quadratic hedging approaches to a high-dimensional setting.

The outline of the paper is the following: in Section 2, we first present the probabilistic setting, a and general market model. To make the discussion self-contained, we devote Section 3 and 4 to a presentation of mean-variance hedging and local risk minimization where we emphasize the link with the BSDEs we intend to numerically solve. Section 5 is where we develop our methodology: we first provide a self-contained introduction to the deep BSDE solver in Section 5.1, and then we apply it in Sections 5.2.1 and 5.2.2 to mean-variance hedging and local risk minimization respectively. Section 6 presents the multi-factor and multi-asset version of the Heston model we use in the numerical experiments and contains some technical proofs that are needed in order to ensure the well-posedness of the mean-variance hedging strategy. Finally, Section 7 is devoted to the numerical experiments while Section 8 concludes the paper.

2 Setting and main assumptions

Let $(\Omega, \mathcal{F}, \mathbb{F}, \mathbb{P})$ a complete filtered probability space, with $\mathbb{F} = \{\mathcal{F}_t\}_{t\geq 0}$ satisfying the usual hypotheses. For $m \geq 1$ and $d \geq 0$, we consider an m-dimensional and a d-dimensional Brownian motion $W_t = (W_t^1, \dots, W_t^m)^\top$ and $B_t = (B_t^1, \dots, B_t^d)^\top$. Throughout the paper we will assume that the filtration $\mathbb{F}$ is generated both by W and B. In particular, the components of W drive the diffusion of the tradable assets, while B models the incompleteness of the market.

Let $q \in \mathbb{N} \setminus \{0\}$. We introduce the following notation:

- $L^2_{\mathcal{F}_T}(\Omega; \mathbb{R}^q)$ is the space of all $\mathcal{F}_T$-measurable $\mathbb{R}^q$-valued random variables $X : \Omega \mapsto \mathbb{R}^q$ such that
$$\|X\|_2 := (\mathbb{E}\,|X|^2)^{1/2} < \infty;$$
- $L^p_{\mathbb{F}}([0,T]; \mathbb{R}^q)$, for $1 \leq p < \infty$, is the space of all $\mathbb{F}$-adapted $\mathbb{R}^q$-valued processes X_t with t in $[0,T]$ such that
$$\|X\|_p := (\mathbb{E}\,[\int_0^T |X_t|^p \,\mathrm{d}t])^{1/p} < \infty;$$
- $L^2_{\mathbb{F}}(\Omega; C([0,T]; \mathbb{R}^q))$ is the space of all $\mathbb{R}^q$-valued $\mathbb{F}$-adapted processes on $[0,T]$ with $\mathbb{P}$-a.s. continuous sample paths such that
$$\mathbb{E}\left[\sup_{t\in[0,T]} |X_t|^2\right] < \infty;$$
- $L^\infty_{\mathbb{F}}(\Omega; C([0,T]; \mathbb{R}^q))$ is the space of all $\mathbb{R}^q$-valued $\mathbb{F}$-adapted essentially bounded processes with continuous sample paths.

2.1 The market model

We consider a financial market with one cash account and m stocks. We denote respectively by S_t^0 and S_t^i the price at time t of the cash account and the i-th stock, with $i = 1, \dots, m$, and

assume their dynamics are given by the following stochastic differential equations (SDEs)

$$\begin{cases} \mathrm{d}S_t^0 = S_t^0 r_t \mathrm{d}t & S_0^0 = 1 \\ \mathrm{d}S_t^i = S_t^i \left[\mu_t^i \mathrm{d}t + \sum_{j=1}^m \sigma_t^{ij} \mathrm{d}W_t^j \right] & S_0^i = s_i, \quad i = 1, \dots, m. \end{cases}, \tag{2.1}$$

where the processes r, μ^i, σ^{ij} $(i, j = 1, \dots, m)$ in $\mathbb{R}$ are $\mathbb{F}$-adapted and are such that existence and uniqueness for solutions to (2.1) is guaranteed. We assume that the short rate of interest r is bounded from below $\mathrm{d}\mathbb{P} \otimes \mathrm{d}t$-a.s.

We remark that the assumption of $\mathbb{F}$-adapted processes in (2.1) covers the case where the coefficients are measurable functions of a set of factors evolving according to additional SDEs: this is the situation which is typically encountered in the context of stochastic volatility models. We also denote by $\mu := (\mu^1, \dots, \mu^m)^\top$ the drift vector and by $\sigma := (\sigma^{ij})_{i,j=1,\dots,m}$ the volatility matrix, which is assumed to be invertible $\mathrm{d}\mathbb{P} \otimes \mathrm{d}t$-a.s.. We set

$$\phi_t := \sigma_t^{-1}(\mu_t - r_t \mathbb{1}).$$

Throughout the paper we mainly work with discounted values. We will use the $\tilde{}$ symbol to denote discounted quantities. In particular, we will denote by $\tilde{S}_t^i := S_t^i / S_t^0$ the discounted stock prices. Clearly, one has

$$\mathrm{d}\tilde{S}_t^i = \tilde{S}_t^i \left[(\mu_t^i - r_t)\mathrm{d}t + \sum_{j=1}^m \sigma_t^{ij} \mathrm{d}W_t^j \right] \qquad \tilde{S}_0^i = s_i, \quad i = 1, \dots, m, \tag{2.2}$$

and $\tilde{S}_t^0 \equiv 1$. We will write $\tilde{S}_t = (\tilde{S}_t^1, \dots, \tilde{S}_t^m)^\top$. Given the assets on the market, an agent may trade on them by constructing a trading strategy.

We introduce the following quantities:

- Let $\xi_t^i \in \mathbb{R}$ be the number of shares of the i-th stock owned by the agent at time t, for $i = 1, \dots, m$, and set $\xi_t := (\xi_t^1, \dots, \xi_t^m)^\top$.
- Let $\psi_t \in \mathbb{R}$ denote the units of the cash account in the agent portfolio at time t.

Assumption 2.1. *We assume that*

1. $(\xi_t)_{t \geq 0}$ *is an* $\mathbb{F}$*-predictable process in* $\mathbb{R}^m$*;*
2. $\mathbb{E}\left[\int_0^T \left| \xi_s^\top \operatorname{diag}(\tilde{S}_s)\sigma_s \right|^2 \mathrm{d}s + \left(\int_0^T \left| \xi_s^\top \operatorname{diag}(\tilde{S}_s)(\mu_s - r_s \mathbb{1}) \right| \mathrm{d}s \right)^2 \right] < \infty,$
   meaning that the stochastic integral $\int_0^T \xi_s^\top \mathrm{d}\tilde{S}_s$ *is well defined in the space of semimartingales. Notice that this comprises the following condition: the process* $(\sigma_t^\top \operatorname{diag}(\tilde{S}_t)\xi_t)_{t \geq 0}$ *belongs to* $L^2_{\mathbb{F}}([0, T]; \mathbb{R}^m)$*;*
3. $(\psi_t)_{t \geq 0}$ *is an* $\mathbb{F}$*-adapted process in* $\mathbb{R}$*.*

Definition 2.1. We call any couple of processes $(\xi, \psi) = (\xi_t, \psi_t)_{t \in [0,T]}$ satisfying the above assumptions a trading strategy and we denote by $\mathcal{A}$ the set of all such strategies.

The (discounted) value process associated to a trading strategy (ξ, ψ) is given by

$$\tilde{V}_t = \sum_{i=1}^m \xi_t^i \tilde{S}_t^i + \psi_t \tilde{S}_t^0 = \sum_{i=1}^m \xi_t^i \tilde{S}_t^i + \psi_t. \tag{2.3}$$

Notice that, for trading strategies satisfying Assumption 2.1, the SDE (2.3) admits a unique strong solution which is a square integrable martingale.

2.2 Self-financing property and financing costs

A fundamental concept to consider when trading is the self-financing property of a strategy.

Definition 2.2. A trading strategy $(\xi, \psi) \in \mathcal{A}$ is *self-financing* if one has

$$\mathrm{d}\tilde{V}_t = \sum_{i=1}^{m} \xi_t^i \mathrm{d}\tilde{S}_t^i, \quad \text{or} \quad \tilde{V}_t = y + \int_0^t \sum_{i=1}^{m} \xi_s^i \mathrm{d}\tilde{S}_s^i,$$

for a given initial wealth $\tilde{V}_0 = y$.

It follows that if the trading strategy is self-financing, $\tilde{V}$ solves the following SDE:

$$\begin{cases} \mathrm{d}\tilde{V}_t = \sum_{i=1}^m \xi_t^i \mathrm{d}\tilde{S}_t^i = \left\{ \sum_{i=1}^m \left[\mu_t^i - r_t\right] \xi_t^i \tilde{S}_t^i \right\} \mathrm{d}t + \sum_{i=1}^m \xi_t^i \tilde{S}_t^i \sum_{j=1}^m \sigma_t^{ij} \mathrm{d}W_t^j, \\ \tilde{V}_0 = y. \end{cases} \tag{2.4}$$

In absence of the self-financing property, a strategy may generate inflows or outflows of cash over time, hence we introduce the following process that monitors such cashflows over time.

Definition 2.3. The (discounted) cumulative cost process $\tilde{C}$ at time t of a strategy $(\xi, \psi) \in \mathcal{A}$ is defined by

$$\tilde{C}_t := \tilde{V}_t - \int_0^t \sum_{i=1}^{m} \xi_s^i \mathrm{d}\tilde{S}_s^i. \tag{2.5}$$

We say that the strategy is mean-self-financing if the process $\tilde{C}$ is a square integrable martingale.

Observe that according with this definition, the cumulative cost for a self-financing strategy coincides with the initial wealth y as it should be.

In the present paper, we are interested in pricing and hedging a (discounted) contingent claim of European type, represented by a positive random variable $\tilde{H} \in L^2_{\mathcal{F}_T}(\Omega; \mathbb{R})$. The random variable $\tilde{H}$ is the unknown payoff at time T, subject to a certain set of market conditions, that is obtained by the holder of the contract. The price paid by the buyer of the contract allows the seller to set up a hedging portfolio to possibly cover the contractual liability at time T. This rather natural approach is at the basis of the study of dynamic trading strategies of the previously announced form (ξ, ψ).

The ideal situation is reached when, by means of an admissible and self-financing trading strategy, the seller/hedger of the contract is able to guarantee the condition $\tilde{V}_T = \tilde{H}$ $\mathbb{P}$-a.s. In this case we say that the claim is attainable and, if all contingent claims are attainable, then the market is said to be complete. In the probabilistic setting we are considering, whenever $d > 0$, the number of Brownian motions is larger than the number of risky assets available for trading. This is a well-known situation where the market is incomplete. Incompleteness means that, for some claims, it will not be possible to construct an admissible self-financing strategy such that $\tilde{V}_T = \tilde{H}$ $\mathbb{P}$-a.s.

For incomplete markets, several approaches to pricing/hedging have been proposed. We can name e.g. utility indifference pricing [5] or superhedging [29]. In the present paper, we focus on the class of quadratic hedging approaches. Within this category, we study both mean-variance hedging and local risk minimization. As perfectly illustrated in [35], such approaches

are defined by relaxing the structure of the set of strategies over which one optimizes investment decisions. In particular:

- If we insist on the fact that strategies should be self-financing, while accepting a tracking error at time T, then we are employing the mean-variance hedging criterion;
- If instead we insist on the idea that $\tilde{V}_T = \tilde{H}$ $\mathbb{P}$-a.s., while accepting that strategies will fail to be self-financing, then we are considering the local risk minimization approach.

In the following we will provide a brief overview of the two hedging approaches we consider. We refer to [35] and references therein for a more formal treatment. In particular we will focus on presenting the link between the hedging approaches and certain BSDEs we would like to solve by means of deep learning methods. Here we consider a single cashflow paid/received at time T, however the concepts we present can be extended to cover the case of streams of cashflows of a contract over the time interval $[0, T]$, see [9] and in particular [36].

3 Mean-variance hedging

The mean-variance hedging approach corresponds to the following stochastic optimal control problem

$$\begin{cases} \inf\limits_{(\xi,\psi)\in\mathcal{A}_{\mathrm{mv}}} \mathbb{E}\left[\left(\tilde{V}_T - \tilde{H}\right)^2 \middle| \mathcal{F}_s\right] \\ \text{subject to (2.4)}, \end{cases} \tag{3.1}$$

where $\mathcal{A}_{\mathrm{mv}}$ denotes the set of admissible trading strategies for problem (3.1) (see Definition 3.1 below). In the following, we use the notation $\tilde{V}^{\mathrm{mv}}$ to stress the fact that the evolution of $\tilde{V}$ is considered in a mean-variance hedging contest. Following the approach of [30], the solution of this problem can be linked to the following system of two BSDEs

$$\begin{cases} \mathrm{d}L_t = \left(|\phi_t|^2 L_t + 2\phi_t^\top \Lambda_{1,t} + \frac{\Lambda_{1,t}^\top \Lambda_{1,t}}{L_t}\right)\mathrm{d}t + \Lambda_{1,t}^\top \mathrm{d}W_t + \Lambda_{2,t}^\top \mathrm{d}B_t \\ L_T = 1 \\ L_t > 0 \end{cases} \tag{3.2}$$

and

$$\begin{cases} \mathrm{d}\tilde{X}_t^{\mathrm{mv}} = \frac{1}{S_t^0}\left(\phi_t^\top \eta_{1,t}^{\mathrm{mv}} - \frac{\Lambda_{2,t}^\top \eta_{2,t}^{\mathrm{mv}}}{L_t}\right)\mathrm{d}t + \eta_{1,t}^{\mathrm{mv},\top}\mathrm{d}W_t + \eta_{2,t}^{\mathrm{mv},\top}\mathrm{d}B_t \\ \tilde{X}_T^{\mathrm{mv}} = \tilde{H} \end{cases}, \tag{3.3}$$

where $\Lambda = (\Lambda_1, \Lambda_2) \in L^2_{\mathbb{F}}\left([0,T]; \mathbb{R}^{m+d}\right)$ and $\eta^{\mathrm{mv}} = (\eta_1^{\mathrm{mv}}, \eta_2^{\mathrm{mv}}) \in L^2_{\mathbb{F}}\left([0,T]; \mathbb{R}^{m+d}\right)$. The set $\mathcal{A}'$ in (3.1) is the set of admissible strategies defined as follows:

Definition 3.1. A trading strategy $(\xi, \psi) \in \mathcal{A}$ is admissible for the mean-variance hedging problem (3.1), if it is self-financing and if the quantity $L_{\tau_k \wedge T}(\tilde{X}^{\mathrm{mv}}_{\tau_k\wedge T} - \tilde{V}^{\mathrm{mv}}_{\tau_k\wedge T})$ is uniformly integrable for any sequence of $\mathbb{F}$-stopping times $\tau_k \nearrow \infty$ as $k \to \infty$.

We state, in a more formal way, the link between the stochastic control problem (3.1) and the system of BSDEs (3.2)-(3.3) via the following result, which closely follows [30, Proposition 3.3].

Proposition 3.1. *If the BSDEs* (3.2) *and* (3.3) *admit unique solutions* $(L, \Lambda) \in L^{\infty}_{\mathbb{F}}(\Omega; C([0,T];\mathbb{R})) \times L^2_{\mathbb{F}}\left([0,T];\mathbb{R}^{m+d}\right)$ *and* $(\tilde{X}^{\mathrm{mv}}, \eta^{\mathrm{mv}}) \in L^2_{\mathbb{F}}(\Omega; C([0,T];\mathbb{R}^m)) \times L^2_{\mathbb{F}}\left([0,T];\mathbb{R}^{m+d}\right)$, *then*

$$\xi^{\mathrm{mv}}_t = \mathrm{diag}(\tilde{S}_t)^{-1}\left(\left(\sigma_t^{-1}\right)^{\top}\left[\phi_t + \frac{\Lambda_{1,t}}{L_t}\right](\tilde{X}^{\mathrm{mv}}_t - \tilde{V}^{\mathrm{mv}}_t) + \left(\sigma_t^{-1}\right)^{\top}\eta^{\mathrm{mv}}_{1,t}\right) \tag{3.4}$$

is the unique optimal control for the stochastic control problem (3.1)*, where* $\tilde{V}^{\mathrm{mv}}$ *is the solution of the SDE* (2.4) *with* $\xi = \xi^{\mathrm{mv}}$.

Proof. See Appendix B. □

Notice that the two BSDEs need to be solved sequentially: first, one solves (3.2) which provides the form of the processes Λ_2 and L appearing in the right-hand side of (3.3).

The first BSDE (3.2) is called *stochastic Riccati equation*: this is a quadratic BSDE for which existence and uniqueness of a solution are non-trivial to prove. For example, [30] provides an existence and uniqueness result based on the work of [28] covering e.g. the Hull-White stochastic volatility case, but his results do not cover, e.g., the Heston model that we consider in Section 7, because of the unboundedness of the coefficients. We shall discuss existence and uniqueness for the particular BSRE we consider in Section 6.1. As shown in [30], the solution to the stochastic Riccati equation characterizes a particular equivalent martingale measure, which is the *variance optimal martingale measure*: this is the pricing measure implicit in the mean-variance hedging approach. More specifically, for $\nu \in L^2_{\mathbb{F}}\left([0,T];\mathbb{R}^d\right)$, the author first defines the exponential local martingale

$$M_{\nu,t} = \exp\left\{-\int_0^t \phi_s^{\top} dW_s - \int_0^t \nu_s^{\top} dB_s - \frac{1}{2}\int_0^t \left(|\phi_s|^2 + |\nu_s|^2\right) ds\right\}. \tag{3.5}$$

If M_ν is a true martingale, one can introduce the parametrized family of measures $\mathrm{d}\mathbb{Q}_\nu = M_{\nu,T}\mathrm{d}\mathbb{P}$ and the variance optimal martingale measure is the measure whose Girsanov kernel for the Brownian motions B solves the following optimization problem

$$\min_{\nu \in L^2_{\mathbb{F}}\left([0,T];\mathbb{R}^d\right)} \mathbb{E}\left[\frac{M_{\nu,T}}{S^0_T}\right]^2. \tag{3.6}$$

The link between the variance optimal martingale measure and the stochastic Riccati equation is presented in Theorem 4.1 in [30]: let ν^{mv} be the solution to the minimization problem (3.6), so that $\mathbb{Q}_{\mathrm{mv}} := \mathbb{Q}_{\nu^{\mathrm{mv}}}$ is the variance optimal martingale measure. If the stochastic Riccati equation (3.2) admits a solution, then

$$\nu^{\mathrm{mv}} = -\frac{\Lambda_2}{L}. \tag{3.7}$$

The interpration of the second BSDE is the following: $\tilde{X}^{\mathrm{mv}}$ represents the dynamics of a portfolio in a fictiously extended financial market. The initial value of $\tilde{X}^{\mathrm{mv}}$ provides the contingent claim price in the mean-variance hedging approach, see Theorem 4.2 in [30] stating that

$$\tilde{X}^{\mathrm{mv}}_t = \mathbb{E}^{\mathbb{Q}_{\mathrm{mv}}}\left[\tilde{H}\middle|\mathcal{F}_t\right].$$

4 Local risk minimisation

As mentioned above, self-financing trading strategies have constant cost equal to the initial wealth $\tilde{V}_0 = y$. To have a self-financing strategy hedging for a contingent claim means that one can guarantee the payment of the claim at time T simply by investing the initial amount $\tilde{V}_0$, whereas using a non-self-financing strategy carries the risk associated to the cost process $\tilde{C}$. We introduce the *risk process* associated to a trading strategy (ξ, ψ) via the following

$$R_t(\xi, \psi) := \mathbb{E}\left[\left(\tilde{C}_T - \tilde{C}_t\right)^2 \middle| \mathcal{F}_t\right]. \tag{4.1}$$

In the approach proposed by [33], one aims at minimizing the *risk process* with respect to *small perturbations* of the trading strategy (ξ, ψ). The concept of small perturbation requires the introduction of several notations that we skip in the present treatment. We limit ourselves to the following description: the idea is to introduce a measure for the increase of quadratic risk as measured by a relative variation of the (4.1) over time partitions (see [36, Equation (1.3)]). Such measure of the increase of quadratic risk over perturbations is employed in Definition 1.5 in [36] to properly introduce the concept of *local risk minimizing strategy*. For our purposes, we will rely on Theorem 1.6 in [36], suitably reformulated for the case of a single final payoff $\tilde{H}$. Such result states the equivalence between local risk minimizing strategies as in the above mentioned Definition 1.5 and strategies that reach the final payoff, while being mean-self-financing with a cost process being a martingale strongly orthogonal to the martingale component of the discounted asset pricess $\tilde{S}$.

Theorem 4.1 (Theorem 1.6 in [36])**.** *The followings are equivalent:*

1. (ξ, ψ) *is local risk minimizing;*
2. (ξ, ψ) *is such that* $\tilde{V}_T = \tilde{H}$*, is mean-self-financing and the cost process* (2.5) *is strongly orthogonal to the martingale component of* $\tilde{S}$*.*

From now on, we will use the second item in the result above as definition of local risk minimizing strategy. From [36, Proposition 5.2], one has that the existence of a locally risk-minimizing strategy $(\xi^{\mathrm{lr}}, \psi^{\mathrm{lr}})$ is equivalent to the existence of the so-called Föllmer-Schweizer (FS) decomposition of the discounted payoff. To be self-contained we report the full proof as it can be found in [36].

Theorem 4.2 (Proposition 5.2 in [36])**.** *The discounted payoff* $\tilde{H}$ *admits a local risk minimizing strategy* (ξ^{lr}, ψ^{lr}) *if and only if* $\tilde{H}$ *admits the representation*

$$\tilde{H} = h_0 + \int_0^T \zeta_t^\top \mathrm{d}\tilde{S}_t + \mathcal{H}_T \tag{4.2}$$

for some $h_0 \in L^2_{\mathcal{F}_0}(\Omega; \mathbb{R})$*,* $\zeta \in \mathbb{R}^m$ *satisfying Assumption 2.1 (1-2) and* $\mathcal{H}$ *a right-continuous, square integrable martingale strongly orthogonal to the martingale component of* $\tilde{S}$*, such that* $\mathcal{H}_0 = 0$*.*

Proof. Given the decomposition (4.2) with $\mathcal{H}$ strongly orthogonal to the martingale component of $\tilde{S}$, the strategy $(\xi^{\mathrm{lr}}, \psi^{\mathrm{lr}})$ defined by

$$\begin{aligned} \xi_t^{\mathrm{lr}} &= \zeta_t, \\ \tilde{V}_t^{\mathrm{lr}} &= h_0 + \int_0^t \zeta_s^\top \mathrm{d}\tilde{S}_s + \mathcal{H}_t, \end{aligned}$$

with $\psi_t^{\mathrm{lr}} = \tilde{V}_t^{\mathrm{lr}} - \sum_{i=1}^m \xi_t^{\mathrm{lr},i}\tilde{S}_t^i$, has the following cost process

$$\tilde{C}_t = \tilde{V}_t^{\mathrm{lr}} - \int_0^t \xi_s^{\mathrm{lr},\top}\mathrm{d}\tilde{S}_s = h_0 + \int_0^t \zeta_s^\top \mathrm{d}\tilde{S}_s + \mathcal{H}_t - \int_0^t \xi_s^{\mathrm{lr},\top}\mathrm{d}\tilde{S}_s = h_0 + \mathcal{H}_t.$$

Hence the cost process is a square integrable martingale strongly orthogonal to the martingale component of $\tilde{S}$. We conclude that the strategy is mean self financing with $\tilde{V}_T = \tilde{H}$, hence it is local risk minimizing. Conversely, if the strategy $(\xi^{\mathrm{lr}}, \psi^{\mathrm{lr}})$ is local risk minimizing, then we can write $\tilde{V}_T = \tilde{H}$ as

$$\tilde{H} = \tilde{V}_T = \tilde{C}_T + \int_0^T \xi_s^{\mathrm{lr},\top}\mathrm{d}\tilde{S}_s = \tilde{C}_0 + \int_0^T \xi_s^{\mathrm{lr},\top}\mathrm{d}\tilde{S}_s + \tilde{C}_T - \tilde{C}_0,$$

and we obtain (4.2) with

$$\begin{aligned} h_0 &= \tilde{C}_0, \\ \zeta &= \xi^{\mathrm{lr}}, \\ \mathcal{H} &= \tilde{C} - \tilde{C}_0, \end{aligned}$$

with $\mathcal{H}$ strongly orthogonal to the martingale component of $\tilde{S}$. □

Equipped with the result above, the objective of identifying a local risk minimizing strategy can be fulfilled by finding the Föllmer-Schweizer decomposition (4.2). To achieve this, two alternative approaches can be found in the literature. On the one side, since we are working in the setting of continuous semimartingales, the Föllmer-Schweizer decomposition can be obtained from the Galtchouk-Kunita-Watanabe decomposition under the *minimal martingale measure*. Here we follow an alternative route by introducing a linear BSDE that we proceed to solve at a later step by means of deep learning methods. The result in full generality is provided by [13, Proposition 1.1], here we follow the analog arguments as in [1].

It is clear that $\tilde{S}$ is a special semimartingale. We introduce a BSDE with terminal condition $\tilde{H}$ and a driver f that we determine in the sequel:

$$\tilde{X}_t^{\mathrm{lr}} = \tilde{H} - \int_t^T \eta_{1,s}^{\mathrm{lr},\top}\mathrm{d}W_s - \int_t^T \eta_{2,s}^{\mathrm{lr},\top}\mathrm{d}B_s + \int_t^T f(s, \tilde{X}_s, \eta_{1,s}^{\mathrm{lr}}, \eta_{2,s}^{\mathrm{lr}})\mathrm{d}s. \tag{4.3}$$

Let $(\tilde{X}^{\mathrm{lr}}, \eta^{\mathrm{lr}}) \in L^2_{\mathbb{F}}(\Omega; C([0,T];\mathbb{R}^m)) \times L^2_{\mathbb{F}}\left([0,T];\mathbb{R}^{m+d}\right)$ be its solution with $\eta^{\mathrm{lr}} := \left(\eta_1^{\mathrm{lr}}, \eta_2^{\mathrm{lr}}\right)$. We assume that the driver f can be chosen such that

$$\int_0^t \xi_s^\top \mathrm{d}\tilde{S}_s = \int_0^t \eta_{1,s}^{\mathrm{lr},\top}\mathrm{d}W_s - \int_0^t f(s, \tilde{X}_s^{\mathrm{lr}}, \eta_{1,s}^{\mathrm{lr}}, \eta_{2,s}^{\mathrm{lr}})\mathrm{d}s.$$

However, from the dynamics (2.2) of $\tilde{S}$ it is clear that

$$\int_0^t \xi_s^\top \mathrm{d}\tilde{S}_s = \int_0^t \xi_s^\top \operatorname{diag}(\tilde{S}_s)\sigma_s \mathrm{d}W_s + \int_0^t \xi_s^\top \operatorname{diag}(\tilde{S}_s)(\mu_s - r_s\mathbb{1})\mathrm{d}s.$$

Since $\tilde{S}$ is a special semimartingale, the decomposition above is unique, meaning that

$$\eta_{1,t}^{\mathrm{lr}} = \operatorname{diag}(\tilde{S}_t)\sigma_t^\top \xi_t, \tag{4.4}$$

$$f(t, \tilde{X}_t^{\mathrm{lr}}, \eta_{1,t}^{\mathrm{lr}}, \eta_{2,t}^{\mathrm{lr}}) = -\eta_{1,t}^{\mathrm{lr},\top}\sigma_t^{-1}(\mu_t - r_t\mathbb{1}) = -\eta_{1,t}^{\mathrm{lr},\top}\phi_t. \tag{4.5}$$

To summarize the discussion, we have the following:

Proposition 4.3. *The Föllmer-Schweizer decomposition of $\tilde{H}$ is given by*

$$\tilde{H} = \tilde{X}_0^{\mathrm{lr}} + \int_0^T \eta_{1,s}^{\mathrm{lr},\top} \left(\mathrm{diag}(\tilde{S}_s)\sigma_s\right)^{-1} \mathrm{d}\tilde{S}_s + \int_0^T \eta_{2,s}^{\mathrm{lr},\top} \mathrm{d}B_s, \tag{4.6}$$

where $(\tilde{X}^{\mathrm{lr}}, \eta^{\mathrm{lr}}) \in L^2_{\mathbb{F}}(\Omega; C([0,T];\mathbb{R}^m)) \times L^2_{\mathbb{F}}\left([0,T];\mathbb{R}^{m+d}\right)$ is the unique solution to the linear BSDE

$$\tilde{X}_t^{\mathrm{lr}} = \tilde{H} - \int_t^T \eta_{1,s}^{\mathrm{lr},\top} \mathrm{d}W_s - \int_t^T \eta_{2,s}^{\mathrm{lr},\top} \mathrm{d}B_s - \int_t^T \eta_{1,s}^{\mathrm{lr},\top} \phi_s \mathrm{d}s. \tag{4.7}$$

Remark 4.1.
1. Equations (4.6) and (4.7) correspond, respectively, to equations (1.17) and (1.18) in [13];
2. We stress that the decomposition is computed under the physical measure $\mathbb{P}$.

We conclude the treatment of local risk minimization with the following corollary.

Proposition 4.4. *Under the preceeding assumptions, the optimal hedging portfolio process $\tilde{X}^{lr}$ admits the following representation*

$$\tilde{X}_t^{\mathrm{lr}} = \mathbb{E}^{\mathbb{Q}_{\mathrm{lr}}}\left[\tilde{H}\middle|\mathcal{F}_t\right], \tag{4.8}$$

where the minimal martingale measure is defined be the following Radon-Nikodym derivative

$$\left.\frac{\mathrm{d}\mathbb{Q}_{\mathrm{lr}}}{\mathrm{d}\mathbb{P}}\right|_{\mathcal{F}_t} := e^{-\int_0^t \phi_s^\top \mathrm{d}W_s - \frac{1}{2}\int_0^t \phi_s^\top \phi_s \mathrm{d}s}. \tag{4.9}$$

Proof. The result follows from the representation of the value process of the linear BSDE (4.7) as a conditional expectation. □

Remark 4.2. It is interesting to compare the pricing approach implicit in the two techniques we are considering: local risk minimization and mean-variance hedging imply two different choices for the pricing measure. In the mean-variance hedging approach we see that both the Brownian motions W and B are transformed by the Girsanov change of measure which depends on the solution of the stochastic Riccati equation because of (3.7). In the local risk minimization approach only the Brownian motion W is transformed: the only requirement on the measure is that $\tilde{S}$ is a martingale, hence the name *minimal martingale measure*.

5 Deep quadratic hedging

In this section we first provide a self-contained presentation of the deep BSDE solver proposed by [12] as it is relevant to our setting. After that, we show how to apply the solver in the context of mean-variance hedging and local risk minimization.

5.1 The deep BSDE solver

To introduce the solver, we will start from a general Forward-Backward stochastic differential equation (FBSDE). Let $(\Omega, \mathcal{F}, \mathbb{P})$ be a probability space rich enough to support an $\mathbb{R}^q$-valued Brownian motion $\mathcal{W} = (\mathcal{W}_t)_{t\in[0,T]}$. Let $\mathbb{F} = (\mathcal{F}_t)_{t\in[0,T]}$ be the filtration generated by $\mathcal{W}$,

assumed to satisfy the standard assumptions. Let us consider an FBSDE in the following general form:

$$\mathcal{X}_t = x + \int_0^t b\left(s, \mathcal{X}_s\right) \mathrm{d}s + \int_0^t a\left(s, \mathcal{X}_s\right) \mathrm{d}\mathcal{W}_s, \quad x \in \mathbb{R}^q, \tag{5.1}$$

$$\mathcal{Y}_t = \vartheta(\mathcal{X}_T) + \int_t^T h\left(s, \mathcal{X}_s, \mathcal{Y}_s, \mathcal{Z}_s\right) \mathrm{d}s - \int_t^T \mathcal{Z}_s^\top \mathrm{d}\mathcal{W}_s, \quad t \in [0,T], \tag{5.2}$$

where the vector fields $b : [0,T] \times \mathbb{R}^q \to \mathbb{R}^q$, $a : [0,T] \times \mathbb{R}^q \to \mathbb{R}^{q \times q}$, $h : [0,T] \times \mathbb{R}^q \times \mathbb{R} \times \mathbb{R}^q \to \mathbb{R}$ and $\vartheta : \mathbb{R}^q \to \mathbb{R}$ satisfy suitable assumptions ensuring existence and uniqueness results.

The FBSDE we consider is intimately linked with the following stochastic control problem:

$$\underset{y,\, \mathcal{Z}=(\mathcal{Z}_t)_{t\in[0,T]}}{\text{minimise}} \quad \mathbb{E}\left[\left|\vartheta(\mathcal{X}_T) - \mathcal{Y}_T\right|^2\right] \tag{5.3}$$

$$\text{subject to } \begin{cases} \mathcal{X}_t &= x + \int_0^t b\left(s, \mathcal{X}_s\right) \mathrm{d}s + \int_0^t a\left(s, \mathcal{X}_s\right) \mathrm{d}\mathcal{W}_s, \\ \mathcal{Y}_t &= y - \int_0^t h\big(s, \mathcal{X}_s, \mathcal{Y}_s, \mathcal{Z}_s\big)\mathrm{d}s + \int_0^t \mathcal{Z}_s^\top \mathrm{d}\mathcal{W}_s, \quad t \in [0,T]. \end{cases} \tag{5.4}$$

More precisely, a solution $(\mathcal{Y}, \mathcal{Z})$ to (5.2) is a minimiser of the problem (5.3).

The idea of the deep BSDE solver is to numerically solve a discretized version of the optimal control problem (5.3)–(5.4). For $N \in \mathbb{N}$, we introduce a time discretization $0 = t_0 < t_1 < \ldots < t_N = T$. Without loss of generality, we consider a uniform mesh with step Δt such that $t_n = n\Delta t$, $n = 0, \ldots, N$, and denote $\Delta\mathcal{W}_n = \mathcal{W}_{t_{n+1}} - \mathcal{W}_{t_n}$. We consider an Euler-Maruyama discretization of the system (5.3)–(5.4), i.e.

$$\overline{\mathcal{X}}_{n+1} = \overline{\mathcal{X}}_n + b(t_n, \overline{\mathcal{X}}_n)\Delta t + a(t_n, \overline{\mathcal{X}}_n)\Delta\mathcal{W}_n, \qquad \overline{\mathcal{X}}_0 = x, \tag{5.5}$$

$$\overline{\mathcal{Y}}_{n+1} = \overline{\mathcal{Y}}_n - h(t_n, \overline{\mathcal{X}}_n, \overline{\mathcal{Y}}_n, \overline{\mathcal{Z}}_n)\Delta t + \overline{\mathcal{Z}}_n^\top \Delta\mathcal{W}_n, \qquad \overline{\mathcal{Y}}_0 = y. \tag{5.6}$$

The deep BSDE solver consists in approximating, at each time step n, the control process $\overline{\mathcal{Z}}_n$ in (5.6) by means of an artificial neural network (ANN), namely by a function $\mathcal{N}_n^{\mathcal{Z}} : \mathbb{R}^q \to \mathbb{R}^q$ of the form $\mathcal{N}_n^{\mathcal{Z}}(x) = \mathcal{L}_\ell^n \circ \varrho \circ \mathcal{L}_{\ell-1}^n \circ \ldots \circ \varrho \circ \mathcal{L}_1^n(x)$, where all $\mathcal{L}_j^n$, for all $j = 1, \ldots, \ell$ and $n = 1, \ldots, N-1$, are affine transformations and ϱ, called *activation function*, is a univariate function that is applied component-wise to vectors. Equation (5.6) then becomes

$$\widehat{\mathcal{Y}}_{n+1} = \widehat{\mathcal{Y}}_n - h(t_n, \overline{\mathcal{X}}_n, \widehat{\mathcal{Y}}_n, \mathcal{N}_n^{\mathcal{Z}})\Delta t + \mathcal{N}_n^{\mathcal{Z},\top} \Delta\mathcal{W}_n, \qquad \widehat{\mathcal{Y}}_0 = y. \tag{5.7}$$

Since we are approximating the control process $\overline{\mathcal{Z}}_n$ at each time step n, we need in practice a family $\left(\mathcal{N}_n^{\mathcal{Z}}\right)_{n=1}^{N-1}$ of ANNs.

By denoting with $\mathcal{P}((\mathcal{N}_n^{\mathcal{Z}})_{n=1}^{N-1})$ the set of all the parameters, i.e. weights and biases, of the ANNs family, the stochastic control problem (5.3) reduces then to

$$\underset{y, \mathcal{P}((\mathcal{N}_n^{\mathcal{Z}})_{n=1}^{N-1})}{\text{minimise}} \quad \mathbb{E}\left[\left|\vartheta(\overline{\mathcal{X}}_N) - \widehat{\mathcal{Y}}_N\right|^2\right]. \tag{5.8}$$

By stochastic gradient descent, the deep BSDE solver trains the ANNs and finds the optimal initial value $\widehat{y}$ and the set of parameters $\mathcal{P}((\widehat{\mathcal{N}}_n^{\mathcal{Z}})_{n=1}^{N-1})$ characterizing the optimal family of networks $(\widehat{\mathcal{N}}_n^{\mathcal{Z}})_{n=1}^{N-1}$.

5.2 Details on the parametrization of the solver

In this section we link the setup of the deep BSDE solver with the market model from Section 2.1. With respect to the general presentation of the solver, we set $q = m + d$ and $\mathcal{W} = (W, B)^\top \in \mathbb{R}^q$. Concerning the forward SDE (5.1), the coefficients appearing in the dynamics of the risky assets are $\mathbb{F}$-measurable, meaning that they will depend in general on both the Brownian motions $W^1, \dots, W^m$ and $B^1, \dots, B^d$. To capture this, we introduce an additional $\mathbb{R}^d$-dimensional risk factor process $Y = (Y_t)_{t\in[0,T]}$ following the dynamics

$$\mathrm{d}Y_t = \gamma(t, Y_t)dt + \Gamma(t, Y_t)\mathrm{d}\mathcal{W}_t, \qquad Y_0 = y_0, \tag{5.9}$$

with $\gamma : [0, T] \times \mathbb{R}^d \to \mathbb{R}^d$ and $\Gamma : [0, T] \times \mathbb{R}^d \to \mathbb{R}^{d\times q}$ of the form $\Gamma = (\Gamma^W, \Gamma^B)$ for Γ^W $\mathbb{R}^{d\times m}$-valued and Γ^B $\mathbb{R}^{d\times d}$-valued. Moreover, the coefficients r, μ^i and $\sigma^{i,j}$ in (2.2) are assumed to be sufficiently regular functions of Y, for $i, j = 1, \dots, m$. We omit such dependence to ease the notation.

The forward process $\mathcal{X}$ in (5.1) collects then both the m risky assets $\tilde{S}^1, \dots, \tilde{S}^m$ in its first m components, and, additionally, the factor process Y, so that $\mathcal{X} = (\tilde{S}^1, \dots, \tilde{S}^m, Y^1, \dots, Y^d)^\top$. From equations (2.2) and (5.9), the precise form of the vector fields in (5.1) is the following: for the diffusion matrix we set

$$a(t, \mathcal{X}_t) = \begin{pmatrix} \mathrm{diag}(\tilde{S}_t)\sigma_t & \mathbf{0} \\ \Gamma^W(t, Y_t) & \Gamma^B(t, Y_t) \end{pmatrix}$$

where $\mathbf{0} \in \mathbb{R}^{m\times d}$ is a matrix of 0's, and, similarly, for the drift term we set

$$b(t, \mathcal{X}_t) = \begin{pmatrix} \mathrm{diag}(\tilde{S}_t)\,(\mu_t - r_t\mathbb{1}) \\ \gamma(t, Y_t) \end{pmatrix}.$$

We assume the newly introduced coefficients γ and Γ to be sufficiently regular so that the SDE satisfied by $\mathcal{X}$ admits a unique strong solution.

The corresponding to the backward process $\mathcal{Y}$ in (5.2) is given, case by case, by the BSDE that the quadratic hedging approach selected require to solve. We shall be more precise about this in the next two paragraphs.

5.2.1 Deep mean-variance hedging

As illustrated in Section 3, there are two BSDEs we need to solve in the mean-variance hedging case. As a first step we discretize (3.2), which is the stochastic Riccati equation parametrizing the variance optimal martingale measure. We get

$$\begin{cases} \overline{L}_{n+1} = \overline{L}_n + \left(|\phi_n|^2\overline{L}_n + 2\phi_n^\top\overline{\Lambda}_{1,n} + \frac{\overline{\Lambda}_{1,n}^\top\overline{\Lambda}_{1,n}}{\overline{L}_n} \right)\Delta t + \overline{\Lambda}_n^\top\Delta\mathcal{W}_n, & \text{for } n = 0, \dots, N-1, \\ \overline{L}_0 = y_L, \end{cases}$$

where $\phi_n = \phi_{t_n}$. Next, in order to apply the solver, we assume that, for each time step n, $\overline{\Lambda}_n^\top = \left(\overline{\Lambda}_{1,n}^\top, \overline{\Lambda}_{2,n}^\top\right)$ is parametrized by an ANN $\mathcal{N}_n^\Lambda$ of the form

$$\mathcal{N}_n^\Lambda = \begin{pmatrix} \mathcal{N}_{1,n}^\Lambda \\ \mathcal{N}_{2,n}^\Lambda \end{pmatrix},$$

with $\mathcal{N}^{\Lambda}_{1,n} : \mathbb{R}^q \mapsto \mathbb{R}^m$ and $\mathcal{N}^{\Lambda}_{2,n} : \mathbb{R}^q \mapsto \mathbb{R}^d$. The discretized BSDE takes then the form

$$\begin{cases} \widehat{L}_{n+1} = \widehat{L}_n + \left(|\phi_n|^2 \widehat{L}_n + 2\phi_n^\top \mathcal{N}^{\Lambda}_{1,n}(\overline{\mathcal{X}}_n) + \frac{\left(\mathcal{N}^{\Lambda}_{1,n}(\overline{\mathcal{X}}_n)\right)^\top \mathcal{N}^{\Lambda}_{1,n}(\overline{\mathcal{X}}_n)}{\widehat{L}_n} \right) \Delta t + \left(\mathcal{N}^{\Lambda}_n(\overline{\mathcal{X}}_n)\right)^\top \Delta \mathcal{W}_n, \\ \qquad\qquad\qquad\qquad\qquad\qquad\qquad\qquad\qquad\qquad\qquad\qquad \text{for } n = 0, \dots, N-1, \\ \widehat{L}_0 = y_L, \end{cases} \tag{5.10}$$

where $\overline{\mathcal{X}}_n$ is the discretized forward process (5.5). As a consequence of the previous approximations, taking into account the terminal condition of the stochastic Riccati BSDE, the stochastic control problem (5.3) involves a minimization over the initial value y_L and the set of parameters of the ANNs that we denote by $\mathcal{P}((\mathcal{N}^{\Lambda}_n)_{n=1}^{N-1})$. We then need to solve

$$\underset{y_L, \mathcal{P}((\mathcal{N}^{\Lambda}_n)_{n=1}^{N-1})}{\text{minimise}} \ \mathbb{E}\left[\left| 1 - \widehat{L}_N \right|^2 \right]. \tag{5.11}$$

We denote by $\widehat{y}_L$ and $(\widehat{\mathcal{N}}^{\Lambda}_n)_{n=1}^{N-1}$ the numerical solution of the above minimization problem obtained via the application of the deep solver. Substituting in equation (5.10) we also get the values of the process $\widehat{L}_n$, for $n = 1, \dots, N$.

Equipped with such numerical solution, we focus now on the portfolio dynamics in the fictiously extended financial market (3.3). Once again, we perform an Euler-Maruyama discretization, meaning that we consider

$$\begin{cases} \overline{X}^{\mathrm{mv}}_{n+1} = \overline{X}^{\mathrm{mv}}_n + \left(\phi_n^\top \overline{\eta}^{\mathrm{mv}}_{1,n} - \frac{\overline{\Lambda}^\top_{2,n} \overline{\eta}^{\mathrm{mv}}_{2,n}}{\overline{L}_n} \right) \Delta t + \overline{\eta}^{\mathrm{mv},\top}_n \Delta \mathcal{W}_n, \qquad \text{for } n = 0, \dots, N-1, \\ \overline{X}^{\mathrm{mv}}_0 = y^{\mathrm{mv}}_X, \end{cases}$$

where $\overline{\eta}^{\mathrm{mv},\top}_n = \left(\overline{\eta}^{\mathrm{mv},\top}_{1,n}, \overline{\eta}^{\mathrm{mv},\top}_{2,n} \right)$. Next, we introduce a second family of ANNs $\mathcal{N}^{\eta^{\mathrm{mv}}}_n : \mathbb{R}^q \mapsto \mathbb{R}^q$ of the form

$$\mathcal{N}^{\eta^{\mathrm{mv}}}_n = \begin{pmatrix} \mathcal{N}^{\eta^{\mathrm{mv}}}_{1,n} \\ \mathcal{N}^{\eta^{\mathrm{mv}}}_{2,n} \end{pmatrix},$$

with $\mathcal{N}^{\eta^{\mathrm{mv}}}_{1,n} : \mathbb{R}^q \mapsto \mathbb{R}^m$ and $\mathcal{N}^{\eta^{\mathrm{mv}}}_{2,n} : \mathbb{R}^q \mapsto \mathbb{R}^d$, depending on the set of parameters, namely weights and biases, that we denote by $\mathcal{P}((\mathcal{N}^{\eta^{\mathrm{mv}}}_n)_{n=1}^{N-1})$. Such networks allow us to introduce the following approximation:

$$\begin{cases} \widehat{X}^{\mathrm{mv}}_{n+1} = \widehat{X}^{\mathrm{mv}}_n + \left(\phi_n^\top \mathcal{N}^{\eta^{\mathrm{mv}}}_{1,n}(\overline{\mathcal{X}}_n) - \frac{\left(\widehat{\mathcal{N}}^{\Lambda}_{2,n}(\overline{\mathcal{X}}_n)\right)^\top \mathcal{N}^{\eta^{\mathrm{mv}}}_{2,n}(\overline{\mathcal{X}}_n)}{\widehat{L}_n} \right) \Delta t + \left(\mathcal{N}^{\eta^{\mathrm{mv}}}_n(\overline{\mathcal{X}}_n) \right)^\top \Delta \mathcal{W}_n, \\ \qquad\qquad\qquad\qquad\qquad\qquad\qquad\qquad\qquad\qquad\qquad\qquad \text{for } n = 0, \dots, N-1, \\ \widehat{X}^{\mathrm{mv}}_0 = y^{\mathrm{mv}}_X, \end{cases} \tag{5.12}$$

where $\widehat{\mathcal{N}}^{\Lambda}_{2,n}$ and $\widehat{L}_n$ are results of the first optimization problem (5.11), for $n = 0, \dots, N-1$. The associated stochastic control problem (5.3) involves a minimization over the initial value y^{mv}_X and the networks' parameters $\mathcal{P}((\mathcal{N}^{\eta^{\mathrm{mv}}}_n)_{n=1}^{N-1})$:

$$\underset{y^{\mathrm{mv}}_X, \mathcal{P}((\mathcal{N}^{\eta^{\mathrm{mv}}}_n)_{n=1}^{N-1})}{\text{minimise}} \ \mathbb{E}\left[\left| \tilde{H} - \widehat{X}^{\mathrm{mv}}_N \right|^2 \right]. \tag{5.13}$$

We denote by $\widehat{y}_X^{\mathrm{mv}}$ and $(\widehat{\mathcal{N}}_n^{\eta^{\mathrm{mv}}})_{n=1}^{N-1}$ the numerical solution of the above minimization problem obtained with a second application of the deep solver. From equation (5.12) we also get the values of the process $\widehat{X}_n^{\mathrm{mv}}$, for $n = 1, \dots, N$.

The approximated optimal trading strategy and the corresponding value process can then be recursively computed starting from equation (2.4) and (3.4) as follows:

$$\begin{cases} \widehat{V}_0^{\mathrm{mv}} = \widehat{y}_X^{\mathrm{mv}} \\ \widehat{\xi}_n^{\mathrm{mv}} = \mathrm{diag}(\overline{S}_n)^{-1} \left(\left(\sigma_n^{-1}\right)^\top \left[\phi_n + \frac{\widehat{\mathcal{N}}_{1,n}^{\Lambda}(\overline{\mathcal{X}}_n)}{\widehat{L}_n} \right] (\widehat{X}_n^{\mathrm{mv}} - \widehat{V}_n^{\mathrm{mv}}) + \left(\sigma_n^{-1}\right)^\top \widehat{\mathcal{N}}_{1,n}^{\eta^{\mathrm{mv}}}(\overline{\mathcal{X}}_n) \right) \\ \widehat{\psi}_n^{\mathrm{mv}} = \widehat{X}_n^{\mathrm{mv}} - \mathrm{diag}(\overline{S}_n)\widehat{\xi}_n^{\mathrm{mv}} \\ \widehat{V}_{n+1}^{\mathrm{mv}} = \widehat{V}_n^{\mathrm{mv}} + \left\{ \sum_{i=1}^m \left[\mu_n^i - r_n\right] \widehat{\xi}_n^{\mathrm{mv}} \overline{S}_n \right\} \Delta t + \sum_{i=1}^m \widehat{\xi}_n^{\mathrm{mv}} \overline{S}_n \sum_{j=1}^m \sigma_n^{ij} \Delta W_n^j \\ \qquad\qquad\qquad\qquad\qquad\qquad\qquad\qquad\qquad\qquad\qquad\qquad \text{for } n = 0, \dots, N-1. \end{cases}$$

5.2.2 Deep local risk minimization

To approximation of local risk minimizing strategies by means of the deep solver poses less challenges with respect to the mean-variance hedging approach. In fact, thanks to Proposition 4.3, we know that to find the Föllmer-Schweizer decomposition we need to solve the linear BSDE (4.7). This, in discretized form, reads like

$$\begin{cases} \overline{X}_{n+1}^{\mathrm{lr}} = \overline{X}_n^{\mathrm{lr}} + \overline{\eta}_{1,n}^{\mathrm{lr},\top} \phi_n \Delta t + \overline{\eta}_n^{\mathrm{lr},\top} \Delta \mathcal{W}_n, \qquad \text{for } n = 0, \dots, N-1, \\ \overline{X}_0^{\mathrm{lr}} = y_X^{\mathrm{lr}}, \end{cases} \tag{5.14}$$

where $\overline{\eta}_n^{\mathrm{lr},\top} = \left(\overline{\eta}_{1,n}^{\mathrm{lr},\top}, \overline{\eta}_{2,n}^{\mathrm{lr},\top}\right)$. We introduce a family of ANNs $\mathcal{N}_n^{\eta^{\mathrm{lr}}} : \mathbb{R}^q \mapsto \mathbb{R}^q$, $n = 0, \dots, N-1$, of the form

$$\mathcal{N}_n^{\eta^{\mathrm{lr}}} = \begin{pmatrix} \mathcal{N}_{1,n}^{\eta^{\mathrm{lr}}} \\ \mathcal{N}_{2,n}^{\eta^{\mathrm{lr}}} \end{pmatrix}$$

with $\mathcal{N}_{1,n}^{\eta^{\mathrm{lr}}} : \mathbb{R}^q \mapsto \mathbb{R}^m$ and $\mathcal{N}_{2,n}^{\eta^{\mathrm{lr}}} : \mathbb{R}^q \mapsto \mathbb{R}^d$. Such networks allow us to introduce the following approximation

$$\begin{cases} \widehat{X}_{n+1}^{\mathrm{lr}} = \widehat{X}_n^{\mathrm{lr}} + \left(\mathcal{N}_{1,n}^{\eta^{\mathrm{lr}}}(\overline{\mathcal{X}}_n)\right)^\top \phi_n \Delta t + \left(\mathcal{N}_n^{\eta^{\mathrm{lr}}}(\overline{\mathcal{X}}_n)\right)^\top \Delta \mathcal{W}_n, \qquad \text{for } n = 0, \dots, N-1, \\ \widehat{X}_0^{\mathrm{lr}} = y_X^{\mathrm{lr}}. \end{cases} \tag{5.15}$$

The associated stochastic control problem (5.3) involves a minimization over the initial value y_X^{lr} and the set of parameters of the ANNs that we denote by $\mathcal{P}((\mathcal{N}_n^{\eta^{\mathrm{lr}}})_{n=1}^{N-1})$:

$$\underset{y_X^{\mathrm{lr}}, \mathcal{P}\left((\mathcal{N}_n^{\eta^{\mathrm{lr}}})_{n=1}^{N-1}\right)}{\text{minimise}} \ \mathbb{E}\left[\left| \tilde{H} - \widehat{X}_N^{\mathrm{lr}} \right|^2 \right]. \tag{5.16}$$

We denote by $\widehat{y}_X^{\mathrm{lr}}$ and $(\widehat{\mathcal{N}}_n^{\eta^{\mathrm{lr}}})_{n=1}^{N-1}$ the numerical solution of the above minimization problem obtained with the deep solver. From equation (5.15) we also get the values of the process $\widehat{X}_n^{\mathrm{lr}}$, for $n = 1, \dots, N$.

The approximated optimal trading strategy can then be computed from (4.4):

$$\begin{cases} \widehat{\xi}_n^{\mathrm{lr}} = \left(\mathrm{diag}(\overline{S}_n)\sigma_n\right)^{-1} \widehat{\mathcal{N}}_{1,n}^{\eta^{\mathrm{lr}}}\left(\overline{\mathcal{X}}_n\right), \\ \widehat{\psi}_n^{\mathrm{lr}} = \widehat{X}_n^{\mathrm{lr}} - \mathrm{diag}(\overline{S}_n)\widehat{\xi}_n^{\mathrm{lr}} \\ \qquad\qquad \text{for } n = 0, \dots, N-1. \end{cases} \tag{5.17}$$

6 The multidimensional Heston model

We shall introduce a multidimensional Heston model that we want to use as the market model [23]. Following the notation of Section 2, we set $m = d$, so that $\tilde{S}, W$ and B are m-dimensional stochastic processes.

Let $A = (A_{ij})_{i,j=1}^m$ be a $m \times m$ matrix of coefficients, and let $\kappa = (\kappa_1, \dots, \kappa_m)^\top$, $\theta = (\theta_1, \dots, \theta_m)^\top$, $\sigma = (\sigma_1, \dots, \sigma_m)^\top$ and $\rho = (\rho_1, \dots, \rho_m)^\top$ be m-dimensional vectors of coefficients with $-1 \le \rho_i \le 1$ for each $i = 1, \dots, m$. We set

$$\begin{aligned} \mu_t &:= A\,\mathrm{diag}(Y_t^2)\bar{\mu} + \bar{r}^\top Y_t^2 \mathbb{1}, \\ r_t &:= \bar{r}^\top Y_t^2 \end{aligned} \tag{6.1}$$

for some $\bar{\mu}, \bar{r} \in \mathbb{R}^m$. We then consider the following system of SDEs

$$\begin{cases} \mathrm{d}\tilde{S}_t^i = \tilde{S}_t^i \left(\sum_{j=1}^m A_{ij} Y_t^{2,j} \bar{\mu}_j \mathrm{d}t + \sum_{j=1}^m A_{ij} Y_t^j \mathrm{d}W_t^j\right), \\ \mathrm{d}Y_t^{2,i} = \kappa_i \left(\theta_i - Y_t^{2,i}\right)\mathrm{d}t + \sigma_i Y_t^i \left(\rho_i \mathrm{d}W_t^i + \sqrt{1-\rho_i^2}\mathrm{d}B_t^i\right), \end{cases} \quad \text{for } i = 1, \dots, m, \tag{6.2}$$

where $Y^j = \sqrt{Y^{2,j}}$. This representation shows that $\tilde{S} = (\tilde{S}^1, \dots, \tilde{S}^m)^\top$ is obtained by combining, by means of the matrix A, all the components of $Y^2 = (Y^{2,1}, \dots, Y^{2,m})^\top$ and of $W = (W^1, \dots, W^m)^\top$. We can also rewrite equation (6.2) in matrix form as

$$\begin{cases} \mathrm{d}\tilde{S}_t = \mathrm{diag}(\tilde{S}_t)\left(\left(A\,\mathrm{diag}(Y_t^2)\bar{\mu}\right)\mathrm{d}t + A\,\mathrm{diag}\left(Y_t\right)\mathrm{d}W_t\right), \\ \mathrm{d}Y_t^2 = \mathrm{diag}(\kappa)\left(\theta - Y_t^2\right)\mathrm{d}t + \mathrm{diag}(\sigma)\mathrm{diag}\left(Y_t\right)\left(\mathrm{diag}(\rho)\mathrm{d}W_t + \mathrm{diag}(\sqrt{\mathbb{1}-\rho^2})\mathrm{d}B_t\right), \end{cases} \tag{6.3}$$

where $\mathrm{diag}(\sqrt{\mathbb{1}-\rho^2})$ denotes the diagonal matrix with diagonal elements $\sqrt{1-\rho_i^2}$, for $i = 1, \dots, m$.

Remark 6.1. 1. The drift of the $\tilde{S}$-dynamics in equation (6.3) is a generalization of the Heston model for the specifications in (6.1), where $A\,\mathrm{diag}(Y_t^2)\bar{\mu} = \mu_t - r_t\mathbb{1}$, for μ and r as in equation (6.1). For $m = 1$ we indeed retrieve a one-dimensional Heston model

$$\begin{cases} \mathrm{d}\tilde{S}_t = \tilde{S}_t\left(\mu Y_t^2 \mathrm{d}t + Y_t \mathrm{d}W_t\right) \\ \mathrm{d}Y_t^2 = \kappa\left(\theta - Y_t^2\right)\mathrm{d}t + \sigma Y_t\left(\rho \mathrm{d}W_t + \sqrt{1-\rho^2}\mathrm{d}B_t\right) \end{cases}, \tag{6.4}$$

with $\bar{\mu} = \bar{\mu}_1 = \mu$ and $A = A_{11} = 1$, where $\mu, \kappa, \theta, \sigma > 0$ are real constants with $-1 \le \rho \le 1$ and $2\kappa\theta > \sigma^2$. In particular, the model (6.4) was proposed by [7] as a modification of the classical Heston model [23]: since they work under a zero interest rate assumption, the market price of risk is then proportional to Y.

2. We notice that the vector process Y^2 in (6.3) is a superposition of Heston-type variances, namely of CIR processes. We then require the Feller condition to hold component-wise,

namely we assume that

$$2\kappa_i\theta_i > \sigma_i^2 \qquad \text{for } i = 1, \dots, m,$$

in order to guarantee (strict) positivity for all the components of Y^2.

3. We also notice that, if A is a diagonal matrix, then $\tilde{S}$ becomes a superposition of mutually independent Heston models of the form of (6.4).

Observe that for the multidimensional Heston model (6.3), according with the notation in Section 5.2, the forward process $\mathcal{X}$ is of the form $\mathcal{X} = (\tilde{S}, Y^2)$ with coefficients

$$a(t, (\tilde{S}_t, Y_t^2)) = \begin{pmatrix} \operatorname{diag}(\tilde{S}_t) A \operatorname{diag}(Y_t) & \emptyset \\ \operatorname{diag}(\sigma) \operatorname{diag}(Y_t) \operatorname{diag}(\rho) & \operatorname{diag}(\sigma) \operatorname{diag}(Y_t) \operatorname{diag}(\sqrt{\mathbb{1} - \rho^2}) \end{pmatrix}$$

where $\emptyset \in \mathbb{R}^{m \times m}$ is a matrix of 0's, and

$$b(t, (\tilde{S}_t, Y_t^2)) = \begin{pmatrix} \operatorname{diag}(\tilde{S}_t) A \operatorname{diag}(Y_t^2) \bar{\mu} \\ \operatorname{diag}(\kappa) \left(\theta - Y_t^2\right) \end{pmatrix}.$$

Similarly for the one-dimensional case (6.4).

6.1 Existence and uniqueness results for the BSRE

The aim of the present section is to prove existence and uniqueness for the stochastic Riccati equation in the case of the multi-dimensional Heston model. We will adapt to our setting the approach of [37]. Let us first notice that, thanks to the assumption (6.1) on the coefficient and diffusion coefficients, straightforward computations show that the market price of risk takes the form

$$\phi_t = \sigma_t^{-1}(\mu_t - r_t \mathbb{1}) = \operatorname{diag}(Y_t)\, \bar{\mu}.$$

Let us also notice that we have $\phi_t^\top \phi_t = \bar{\mu}^\top \operatorname{diag}\left(Y_t^2\right) \bar{\mu} = \bar{\mu}^{2,\top} Y_t^2$, where $\bar{\mu}^2$ denotes a vector where each component is of the form $\bar{\mu}_j^2$, $j = 1, \dots, m$. As a first step, following [37], we obtain a closed-form solution for a solution to the BSRE, which we generalize to the multi-dimensional case.

Lemma 6.1. *Under assumption* (6.1)*, a solution to the stochastic Riccati equation* (3.2) *is given by*

$$L_t = \exp\left\{\varphi(t,T) + \psi(t,T)^\top Y_t^2\right\}, \tag{6.5}$$

where φ, ψ satisfy the following system of Riccati ODEs:

$$\begin{aligned} &\frac{\partial \varphi}{\partial t} + \psi(t,T)^\top \operatorname{diag}(\kappa)\, \theta = 0, \quad \varphi(T,T) = 0, \\ &\frac{\partial \psi}{\partial t}^\top - \psi(t,T)^\top \operatorname{diag}(\kappa) + \frac{1}{2}\psi(t,T)^\top \operatorname{diag}\left(\sigma^2\right) \operatorname{diag}(\psi(t,T)) - \bar{\mu}^{2,\top} \\ &\qquad - 2\psi(t,T)^\top \operatorname{diag}(\sigma) \operatorname{diag}(\rho) \operatorname{diag}(\bar{\mu}) \\ &\qquad - \psi(t,T)^\top \operatorname{diag}\left(\sigma^2\right) \operatorname{diag}\left(\rho^2\right) \operatorname{diag}(\psi(t,T)) = 0, \quad \psi(T,T) = 0. \end{aligned} \tag{6.6}$$

Proof. We apply the Itô formula to (6.5) and write

$$\begin{aligned}
\mathrm{d}L_t &= \frac{\partial L_t}{\partial t} + \frac{\partial L_t}{\partial Y_t^2}\mathrm{d}Y_t^2 + \frac{1}{2}\frac{\partial^2 L_t}{\partial (Y_t^2)^2}\mathrm{d}\left\langle Y^2, Y^2\right\rangle_t \\
&= \left(\frac{\partial \varphi}{\partial t} + \frac{\partial \psi^\top}{\partial t} Y_t^2\right) L_t \mathrm{d}t + L_t \psi(t,T)^\top \left(\mathrm{diag}(\kappa)\left(\theta - Y_t^2\right)\mathrm{d}t \right. \\
&\qquad \left. + \mathrm{diag}(\sigma)\mathrm{diag}\left(Y_t\right)\left(\mathrm{diag}(\rho)\mathrm{d}W_t + \mathrm{diag}(\sqrt{\mathbb{1}-\rho^2})\mathrm{d}B_t\right)\right) \\
&\quad + \frac{1}{2} L_t \psi(t,T)^\top \mathrm{diag}\left(\sigma^2\right)\mathrm{diag}\left(Y_t^2\right)\psi(t,T)\mathrm{d}t \\
&= L_t \overbrace{\left(\frac{\partial \varphi}{\partial t} + \psi(t,T)^\top \mathrm{diag}(\kappa)\theta\right)}^{=0}\mathrm{d}t + L_t \left(\frac{\partial \psi^\top}{\partial t} - \psi(t,T)^\top \mathrm{diag}(\kappa)\right. \\
&\quad \left. + \frac{1}{2} L_t \psi(t,T)^\top \mathrm{diag}\left(\sigma^2\right)\mathrm{diag}\left(\psi(t,T)\right)\right) Y_t^2 \mathrm{d}t + \Lambda_{1,t}^\top \mathrm{d}W_t + \Lambda_{2,t}^\top \mathrm{d}B_t,
\end{aligned}$$

where we defined

$$\begin{aligned}
\Lambda_{1,t}^\top &:= \psi(t,T)^\top \mathrm{diag}\left(\sigma\right)\mathrm{diag}\left(Y_t\right)\mathrm{diag}\left(\rho\right) L_t, \\
\Lambda_{2,t}^\top &:= \psi(t,T)^\top \mathrm{diag}\left(\sigma\right)\mathrm{diag}\left(Y_t\right)\mathrm{diag}\left(\sqrt{\mathbb{1}-\rho^2}\right) L_t.
\end{aligned} \tag{6.7}$$

Concentrating on the drift term, we observe that

$$\begin{aligned}
& L_t \left(\frac{\partial \psi^\top}{\partial t} - \psi(t,T)^\top \mathrm{diag}(\kappa)\right. \\
&\quad \left. + \frac{1}{2} L_t \psi(t,T)^\top \mathrm{diag}\left(\sigma^2\right)\mathrm{diag}\left(\psi(t,T)\right)\right) Y_t^2 \pm \phi_t^\top \phi_t L_t \pm 2\phi_t^\top \Lambda_{1,t} \pm \frac{\Lambda_{1,t}^\top \Lambda_{1,t}}{L_t} \\
&= \phi_t^\top \phi_t L_t + 2\phi_t^\top \Lambda_{1,t} + \frac{\Lambda_{1,t}^\top \Lambda_{1,t}}{L_t},
\end{aligned}$$

due to (6.6), hence the proof is complete. □

Remark 6.2. It is immediate to observe that we can write the vector Riccati ODE in (6.6) as a vector of scalar Riccati ODEs that can be solved independently of each other, namely

$$\frac{\partial \psi_j}{\partial t} - \psi_j(t,T)\kappa_j + \frac{1}{2}\psi_j^2(t,T)\sigma_j^2 - \bar{\mu}_j^2 - 2\psi_j(t,T)\sigma_j\rho_j\bar{\mu}_j - \psi_j^2(t,T)\sigma_j^2\rho_j^2 = 0, \tag{6.8}$$

meaning that one can resort to a standard existence and uniqueness result for the scalar case.

In the next step, we state a standard result on existence and uniqueness on the Riccati system (6.8).

Lemma 6.2. *Let us assume that $\rho_j^2 < \frac{1}{2}$ for all $j = 1, \dots, m$. Then, there exists a unique solution $\psi_j(\cdot, T)$ to the Riccati ODE (6.8) with $\sup_{0\le t\le T}|\psi_j(t,T)| < \infty$. Moreover $\psi_j(t,T) \le 0$ for all $t \in [0,T]$.*

Proof. The result follows from e.g. Lemma 10.12 in [14] by setting, in his notation, $A = \sigma_j^2\left(\frac{1}{2} - \rho_j^2\right)$, $B = -(\kappa_j + 2\bar{\mu}_j\sigma_j\rho_j)$, $C = \bar{\mu}_j^2$, and by applying the change of variable $t \mapsto T - t$. The condition $A > 0$ holds true if and only if $\rho_j^2 < \frac{1}{2}$. We also need to check $C^2 > 0$, but this is trivially true. Finally we need to check that $B^2 + 4AC \in \mathbb{C} \setminus \mathbb{R}_-$, which is also trivially satisfied. □

We can now prove uniqueness by adapting to our setting the approach of [37].

Proposition 6.3. *The triple* $(L, \Lambda_1, \Lambda_2)$ *as provided in* (6.5), (6.6) *and* (6.7) *is the unique solution to the BSRE* (3.2).

Proof. Define $\mathscr{L} := \log L$ and $Z_i := \frac{\Lambda_i}{L}$, $i \in \{1, 2\}$. An application of the Itô formula shows that

$$\mathrm{d}\mathscr{L}_t = \left(|\phi_t|^2 + 2\phi_t^\top Z_{1,t} + \frac{1}{2}|Z_{1,t}|^2 - \frac{1}{2}|Z_{2,t}|^2 \right) \mathrm{d}t + Z_{1,t}^\top \mathrm{d}W_t + Z_{2,t}^\top \mathrm{d}B_t.$$

Let us introduce the measure $\tilde{\mathbb{P}}$ defined via

$$\left.\frac{\partial \tilde{\mathbb{P}}}{\partial \mathbb{P}}\right|_{\mathcal{F}_T} := \exp\left\{ -2\int_0^T |\phi_t|^2 \mathrm{d}t - 2\int_0^T \phi_t^\top \mathrm{d}W_t \right\},$$

which is a true martingale thanks to a component-wise application of Theorem 2.1 in [32]. Under $\tilde{\mathbb{P}}$, $\mathscr{L}$ has dynamics

$$\mathrm{d}\mathscr{L}_t = \left(|\phi_t|^2 + \frac{1}{2}|Z_{1,t}|^2 - \frac{1}{2}|Z_{2,t}|^2 \right) \mathrm{d}t + Z_{1,t}^\top \mathrm{d}\tilde{W}_t + Z_{2,t}^\top \mathrm{d}\tilde{B}_t.$$

We introduce then a second measure change defined via

$$\left.\frac{\partial \check{\mathbb{P}}}{\partial \tilde{\mathbb{P}}}\right|_{\mathcal{F}_T} := \exp\left\{ -\frac{1}{2}\int_0^T |Z_t|^2 \mathrm{d}t - \int_0^T Z_{1,t}^\top \mathrm{d}\tilde{W}_t + \int_0^T Z_{2,t}^\top \mathrm{d}\tilde{B}_t \right\},$$

which is a true martingale due to the boundedness of ψ_j $j = 1, \ldots, m$, allowing us to apply Corollary A1 in [37]. The dynamics of $\mathscr{L}$ under $\check{\mathbb{P}}$ are given by

$$\mathrm{d}\mathscr{L}_t = \left(|\phi_t|^2 + \frac{1}{2}|Z_{1,t}|^2 - \frac{1}{2}|Z_{2,t}|^2 - |Z_{1,t}|^2 + |Z_{2,t}|^2 \right) \mathrm{d}t + Z_{1,t}^\top \mathrm{d}\check{W}_t + Z_{2,t}^\top \mathrm{d}\check{B}_t.$$

We now proceed by contradiction. Assume there are two solutions $(\mathscr{L}, Z)$ and $(\mathscr{L}', Z')$, define $(\Delta\mathscr{L}, \Delta Z) = (\mathscr{L} - \mathscr{L}', Z - Z')$. Under the measure $\check{\mathbb{P}}$ we have

$$\mathrm{d}\Delta\mathscr{L}_t = \left(-\frac{1}{2}|\Delta Z_{1,t}|^2 + \frac{1}{2}|\Delta Z_{2,t}|^2 \right) \mathrm{d}t + \Delta Z_{1,t}^\top \mathrm{d}\check{W}_t + \Delta Z_{2,t}^\top \mathrm{d}\check{B}_t,$$

which is a quadratic BSDE for which there exists a unique solution thanks to the results of [28]. Such solution is given by $(0, \mathbf{0})$ with $\mathbf{0} \in \mathbb{R}^{d+m}$. This implies $\mathscr{L} = \mathscr{L}'$, $Z_1 = Z_1'$ and $Z_2 = Z_2'$ which is a contradiction, hence the solution to the BSRE is unique. □

7 Numerical experiments

We present here the numerical results for mean-variance hedging and local risk minimization under the multidimensional Heston model in Section 6, by means of the deep BSDE solver in Section 5.1. The code for our experiments is available at `https://github.com/silvialava/Deep_quadratic_hedging.git`.

Given a portfolio of $m \geq 1$ risky assets, for a strike price K and a terminal time T, we aim at hedging and pricing a European type call option, whose payoff function $g : \mathbb{R}_+^m \to \mathbb{R}_+$ is of

the form

$$g(x) := \max\left(\sum_{i=1}^{m} x_i - mK, 0\right) \quad \text{for } x \in \mathbb{R}_+^m \text{ with } x = (x_1, \dots, x_m)^\top,$$

so that the discounted contingent claim $\tilde{H}$ becomes

$$\tilde{H} = e^{-\int_0^T r_s \mathrm{d}s} \max\left(\sum_{i=1}^{m} S_T^i - mK, 0\right). \tag{7.1}$$

In the one-dimensional case (6.4), semi-explicit solutions can be computed by following [7] for the mean-variance hedging and [22] for the local risk minimization. We briefly present the two approaches in Appendix A as we shall use them as benchmarks for the deep BSDE solver. Both [7] and [22] rely on a two-dimensional partial differential equation (PDE) which we solve by adapting [25], see Appendix C for details. These allow us to compare the entire contingent claim price path, as well as the trading strategies paths in $[0, T]$.

For higher values of m (indicatively $m \geq 2$), however, solving these PDEs is not numerically feasible. To test the accuracy of the deep BSDE solver one can alternatively perform a change of measure as illustrated, respectively, in (3.5) and (4.9), and estimate the contingent claim price via Monte Carlo simulations under the variance optimal martingale measure and the minimal martingale measure, respectively.

However, from equations (3.5) and (3.7), we observe that the Radon-Nikodym derivative for the change of measure from $\mathbb{P}$ to the optimal martingale measure $\mathbb{Q}_{\mathrm{mv}}$ depends on the solution of the stochastic Riccati equation (3.2), hence it depends on the optimal solution that is found with the deep solver, see Section 5.2.1. Using this approximated density for Monte Carlo simulations under $\mathbb{Q}_{\mathrm{mv}}$ would then lead to biased results.

To overcome this issue, we shall consider for all the experiments a model where the matrix A is diagonal. As pointed out in Remark 6.1, this leads to an $\tilde{S}$ being the superposition of mutually independent Heston models. We then apply component-wise to the vector processes $\tilde{S}$ and Y^2 the change of measure proposed by [7, Section 4] for the one-dimensional Heston model and presented in equation (A.6), and we run the Monte Carlo routine by simulating $\tilde{S}$ and Y^2 directly under the variance optimal martingale measure $\mathbb{Q}_{\mathrm{mv}}$.

On the other hand, for the minimal martingale measure $\mathbb{Q}_{\mathrm{lr}}$, the Radon-Nikodym derivative (4.9) only depends on the market price of risk ϕ. Then either we simulate under $\mathbb{P}$ and multiply by the density process (4.9), or we simulate directly under $\mathbb{Q}_{\mathrm{lr}}$ by performing the corresponding change of measure, namely

$$\begin{aligned} \mathrm{d}W_t^{\mathrm{lr}} &= \mathrm{d}W_t + \phi_t \mathrm{d}t \\ \mathrm{d}B_t^{\mathrm{lr}} &= \mathrm{d}B_t \end{aligned}, \tag{7.2}$$

which, in the multi-dimensional Heston model (6.3), leads to

$$\begin{cases} \mathrm{d}\tilde{S}_t = \mathrm{diag}(\tilde{S}_t) A \,\mathrm{diag}\,(Y_t)\, \mathrm{d}W_t^{\mathrm{lr}}, \\ \mathrm{d}Y_t^2 = \mathrm{diag}(\kappa)\left(\theta - Y_t^2\right)\mathrm{d}t - \mathrm{diag}(\sigma)\mathrm{diag}\,(Y_t)\,\mathrm{diag}(\rho)\phi_t \mathrm{d}t \\ \qquad\qquad + \mathrm{diag}(\sigma)\mathrm{diag}\,(Y_t)\left(\mathrm{diag}(\rho)\mathrm{d}W_t^{\mathrm{lr}} + \mathrm{diag}(\sqrt{\mathbb{1} - \rho^2})\mathrm{d}B_t^{\mathrm{lr}}\right). \end{cases} \tag{7.3}$$

Without loss of generality, for all the experiments we set $\bar{r} \equiv 0$ in equation (6.1), so that the risk-free interest rate is $r_t = 0$ for each $t \geq 0$.

Model configuration		**Deep solver configuration**	
m	$1, 5, 20, 100$	N	$10, 50, 100$
A	$\text{diag}(\mathbb{1})$	Number of layers	4
$\bar{\mu}$	$0.1 \cdot \mathbb{1}$	Number of nodes	$2m + 20$
κ	$0.5 \cdot \mathbb{1}$	Activation function	ReLU
θ	$0.05 \cdot \mathbb{1}$	Total iterations	8000
σ	$0.1 \cdot \mathbb{1}$	Partial iterations	4000
ρ	$-0.45 \cdot \mathbb{1}$	Initial learning rate	$5 \cdot 10^{-2}$
$\tilde{S}_0$	$100.0 \cdot \mathbb{1}$	Second learning rate	$5 \cdot 10^{-3}$
Y_0^2	$0.025 \cdot \mathbb{1}$	y_L initial range	$[0.5, 2.0]$
K	100.0	y_X initial range	MC $\cdot[0.95, 1.05]$
T	1.0	Batch size	128

Table 1: Model configuration and deep solver configuration for the numerical experiments.

7.1 Setup

We conduct several numerical experiments on the multivariate Heston model to test the performances of the deep BSDE solver for quadratic hedging: both model and solver configuration details are in Table 1, where $\mathbb{1} \in \mathbb{R}^m$ denotes a vector of 1's.

In particular, we consider four different portfolio dimensions, respectively $m = 1, 5, 20, 100$. As we already mentioned above, the matrix A is taken to be diagonal: this allows us to simulate under the variance optimal martingale measure by performing for each risky asset a uni-dimensional change of measure as in (A.6). Moreover, we consider all the model parameters to be constant vectors, so that also the one-dimensional case fits smoothly into the setting. We fix the strike price to $K = 100.0$ and the terminal time is $T = 1.0$

We consider three different discretization grids, respectively $N = 10$, $N = 50$ and $N = 100$, which means we have $N = 10, 50, 100$ neural networks that must be trained. Each of them is built with 4 inner layers, where each layer has a number of nodes depending on the portfolio dimension, namely $2m + 20$, and with the rectified linear unit (ReLU) as activation function. For the training of the neural networks, we set to 8000 the total number of stochastic gradient descent iterations with initial learning rate equal to $5 \cdot 10^{-2}$. After 4000 iterations (Partial iteration), the learning rate is reduced to $5 \cdot 10^{-3}$ to improve the convergence of the method.

Finally, we need to define an initial guess for y_L and y_X^{mv} for the deep mean-variance hedging, see Section 5.2.1, and an initial guess for y_X^{lr} for the deep local risk minimization, see Section 5.2.2. Since we know that $0 < L \leq 1$, we set the range for y_L to $[0.5, 2.0]$, while for y_X we consider, respectively, the 95% and the 105% of the corresponding Monte Carlo price simulation (MC).

We stress the fact that both model and solver configurations are kept constant in all the experiments, unless explicitly stated. This allows to compare the performance of the BSDE solver consistently. However, we point out that one can aim at improving even further our numerical results by tuning the hyper-parameters of the deep solver in a tailor-made manner for each single experiment.

7.2 Deep mean-variance hedging results

The numerical results for the deep mean-variance hedging approach are presented in Table 2, and in Figure 1 we show the evolution of the logarithmic loss as a function of the deep solver iterations. Here the black curves represent the log-loss for the first BSDE and follow the black

grid on the left-hand side. The red curves represent the log-loss for the second BSDE and follow the red grid on the right-hand side.

For each portfolio dimension considered, we compute the Monte Carlo (MC) price by simulating 10^5 samples with 100 points of time discretization under the variance optimal martingale measure as presented in equation (A.6). Moreover, we compute the initial value of the opportunity process L (L value in the table) by means of formula (A.1) together with equations (A.2) and (A.3). For $t = 0$, L_0 is indeed purely deterministic and, in the one-dimensional case, the value given by (A.1) can be considered the exact value for the opportunity process. In the multidimensional case, since the vector Y^2 is a superposition of mutually independent processes, we can compute the value of L as the products of the m values that one would get if computing L for each uni-dimensional component. In other words, we consider

$$L_0 = \prod_{i=1}^{m} \exp\left(\chi_0^i(0) + \chi_1^i(0) Y_0^{2,i}\right),$$

where each χ_0^i and χ_1^i is computed as in equations (A.2) and (A.3), for $i = 1, \ldots, m$.

We then train and run the BSDE solver for solving recursively the two BSDEs as in Section 5.2.1, obtaining, respectively, an estimate of the initial value of the opportunity process (BSDE solver L value) and an estimate of the call option price (BSDE solver price). For both of them, we report the training time and the relative error, which is computed in the standard way starting from the previously simulated L value and MC price. For the portfolio in dimension 1, we also compute the option price with the Černý and Kallsen approach in [7] (see Section A.1) and the corresponding relative error.

From Table 2 we observe that in all the experiments (except for the two corresponding to $m = 100$ with $N = 50$ and $N = 100$ which we shall comment later) the accuracy for the process L is in the third or forth decimal, and the error for the option price is always below 1%. These results are confirmed by the evolution of the logarithmic loss in Figure 1. We observe indeed that the BSDE solver losses for the first equation (black curves) are in average of the order of 10^{-20}. Different picture appears for the BSDE solver losses for the second equation (red curves) where we observe values of positive order. However, one needs to take into account that the loss is computed in the form of absolute value, and not as a relative value. For the first BSDE, the value of L to be found is between 0 and 1, but for the second BSDE the value of X to be found is of the order of 10^2 (since we take $\tilde{S}_0 = K = 100$) and is expected to grow with the dimension of the problem (because of the contingent claim definition (7.1)). For these reasons, we observe the log-loss increasing with m and, most importantly, not converging to 0 as one may expect.

Exception is made for the two experiments with portfolio dimension $m = 100$ and time grid $N = 50$ and $N = 100$. Here the relative error for the option price is between 1% and 2%. Remember that in the mean-variance hedging the second BSDE depends on the solution of the first BSDE. In these two cases, the solver is failing to solve the first BDSE as we can notice from the values obtained for L (BSDE solver L value) which exhibit a significant discrepancy with respect to the true solution. Quite surprisingly, the error for the second BSDE is still relatively low (below 2%).

By observing the log-loss behavior in these two cases, we see that the solver does not converge for the first BSDE. We then rerun the experiments by decreasing the initial learning rate to $1 \cdot 10^{-3}$ and the second learning rate to $5 \cdot 10^{-4}$. The results are in Figure 2. We see that the new results are in line with all the rest, and the log-loss is now converging as expected.

For the portfolio of dimension 1, we also compute the call option price and hedging strategies evolution, namely units of cash account and shares of risky asset, both with the BSDE approach

and with the approach in [7]. We report them in Figure 3, 4 and 5, respectively for $N = 10$, $N = 50$ and $N = 100$. We observe that not only the solver is capturing the option price path, but also provides good approximated hedging strategies.

To have a clearer picture of the solver performance when the number of time steps is increased, we report in Figure 10 the Mean Squared Error (MSE) as a function of time for the option price, for the units of cash account and for the shares of risky asset in dimension one. For the option price, we observe that the MSE is increasing with time. However, we also see a clear improvement when increasing the number of time steps, N. This means that, despite the error is accumulating over time, one can still control it by decreasing the mesh size in the time discretization.

We do not observe the same clear behavior for the units of cash account and the shares of risky asset. However, we point out that, while the optimization is done to approximate the BSDE, hence to approximate the option price process, the strategies are in some sense a by-product of such optimization. So the fact that the MSE in these two cases is not monotone is to be expected. For these reasons, we also report as a dashed line the mean over time of the MSE. Here we observe that the mean of MSE decreases from $N = 10$ to $N = 50$, while the line corresponding to $N = 100$ is not visible because overlapping with the $N = 50$ one. For the sake of completeness, we report here their values: for the units of cash accounts, the mean MSE for $N = 50$ is $5.33 \cdot 10^{-4}$ and the mean MSE for $N = 100$ is $6.73 \cdot 10^{-4}$; for the shares of risky asset, the mean MSE for $N = 50$ is $4.92 \cdot 10^{-4}$ and the mean MSE for $N = 100$ is $6.44 \cdot 10^{-4}$. Hence it gets slightly worse for $N = 100$. We point out that when N increases one has a higher number of ANNs to train, so that the same number of iterations used for lower values of N may be not sufficient to guarantee an improvement of the results.

7.3 Deep local risk minimization results

The numerical results for the deep local risk minimization are presented in Table 3, and in Figure 6 we show the evolution of the logarithmic loss as a function of the deep solver iterations.

As before, for each portfolio dimension we compute the Monte Carlo (MC) price by simulating 10^5 samples with 100 points of time discretization under the minimal martingale measure as presented in (7.3). We then train and run the solver for solving the BSDE as in Section 5.2.2, obtaining an estimate of the call option price (BSDE solver price). We report the training time and the relative error, which is computed in the standard way starting from the previously simulated MC price. For the portfolio in dimension 1, we also compute the option price with the Heath, Platen and Schweizer approach presented in Section A.2 and the corresponding relative error.

From Table 3 we observe that in all the experiments the error for the option price is below 1.5%, and in particular below 1% for $N = 50$ and $N = 100$. Clear convergence is also confirmed by the evolution of the logarithmic loss in Figure 6.

For the portfolio of dimension 1, we compute the call option price and hedging strategies evolution, namely units of cash account and shares of risky asset, both with the BSDE approach and with the Heath, Platen and Schweizer approach. We report them in Figure 7, 8 and 9, respectively for $N = 10$, $N = 50$ and $N = 100$. We observe that the solver is capturing well the paths of the option price, of the units and of the shares.

A more complete picture is given by the MSE in Figure 10. Here we indeed observe that for the option price the MSE accumulates over time, but is clearly decreasing with the number of time steps, N, hence the error can be controlled by decreasing the mesh size in the time discretization. Less clear is the situation for the units of cash account and the shares of risky asset. However, the dashed lines representing the mean over time of the MSE show that also

Mean-variance hedging

Portfolio dimension: 1		**MC price:**	**6.837**
		***L* value:**	**0.99984**
Time steps	**10**	**50**	**100**
BSDE solver *L* value	0.99969	0.99970	0.99969
Relative error (%)	0.01476	0.01434	0.01493
1st training time (s)	82	576	1048
BSDE solver price	**6.830**	**6.854**	**6.838**
Relative error (%)	**0.105**	**0.246**	**0.0250**
2nd training time (s)	1015	3270	5785
PDE price	6.853	6.853	6.853
Relative error (%)	0.245	0.233	0.232
Portfolio dimension: 5		**MC price:**	**15.298**
		***L* value:**	**0.99848**
Time steps	**10**	**50**	**100**
BSDE solver *L* value	0.99848	0.99848	0.99848
Relative error (%)	0.00028	0.00040	0.00019
1st training time (s)	384	2360	3830
BSDE solver price	**15.329**	**15.363**	**15.383**
Relative error (%)	**0.201**	**0.422**	**0.554**
2nd training time (s)	1702	6065	10345
Portfolio dimension: 20		**MC price:**	**30.560**
		***L* value:**	**0.99393**
Time steps	**10**	**50**	**100**
BSDE solver *L* value	0.99401	0.99396	0.99394
Relative error (%)	0.00797	0.00335	0.00140
1st training time (s)	1396	9547	5763
BSDE solver price	**30.612**	**30.788**	**30.800**
Relative error (%)	**0.171**	**0.748**	**0.786**
2nd training time (s)	7704	13843	28510
Portfolio dimension: 100		**MC price:**	**68.831**
		***L* value:**	**0.97002**
Time steps	**10**	**50**	**100**
BSDE solver *L* value	0.97044	0.12426	0.27013
Relative error (%)	0.02936	87.19	72.15
1st training time (s)	1757	9860	20917
BSDE solver price	**68.168**	**69.720**	**67.602**
Relative error (%)	**0.964**	**1.291**	**1.706**
2nd training time (s)	4516	21843	40253

Table 2: Mean-variance hedging results for different portfolio dimensions and different number of total time steps in the discretization grid. For each configuration, we compute the Monte Carlo (MC) price by simulating 10^5 samples under the variance optimal martingale measure, and we use it to compute the relative error in the classical way. For the portfolio with only one risky asset, we report the price obtained with the benchmark approach via PDE presented in Appendix A.1.

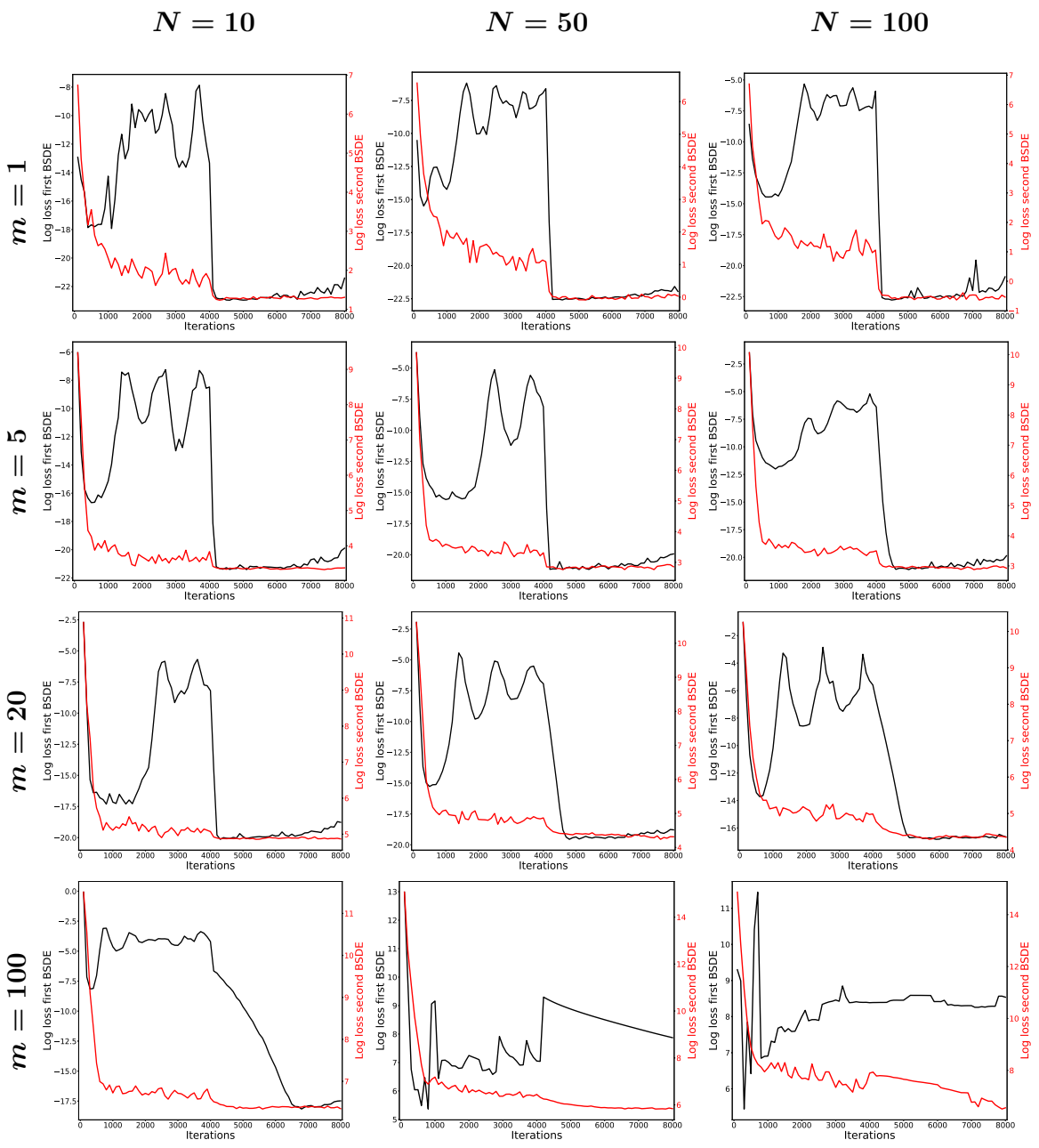

Figure 1: Logarithm of the loss functional as a function of the iteration number for the different experiment configurations presented in Table 2. The black curves represent the log-loss for the first BSDE and follow the black grid on the left-hand side. The red curves represent the log-loss for the second BSDE and follow the red grid on the right-hand side.

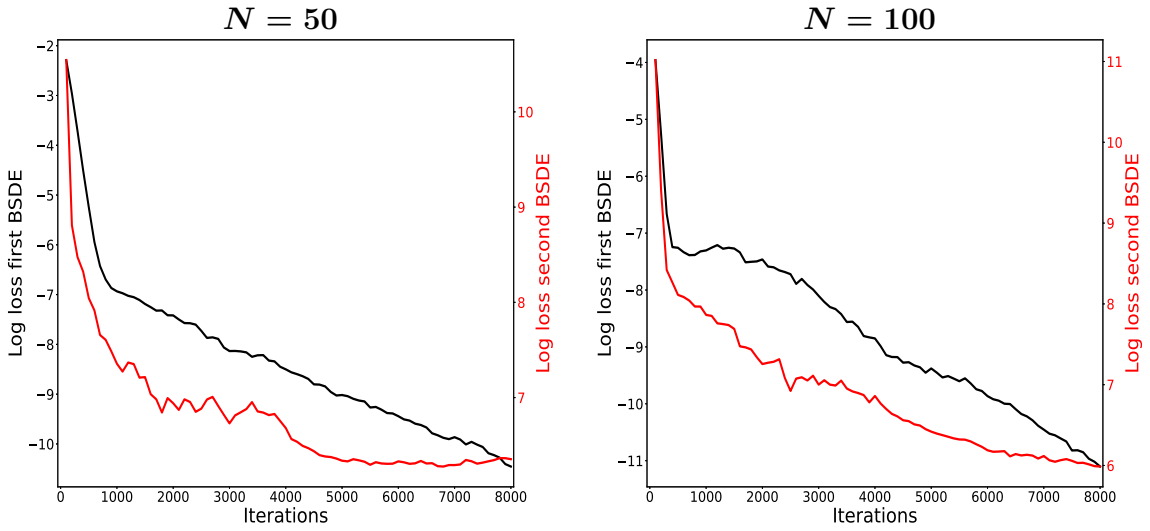

BSDE solver L value: 0.97007 (0.00489 %)
BSDE solver price: 68.892 (0.0878 %)

BSDE solver L value: 0.97024 (0.0230 %)
BSDE solver price: 68.910 (0.114 %)

Figure 2: Mean-variance hedging results with portfolio dimension $m = 100$, when we reduce the learning rates values and improve the experiments in Table 2 and Figure 1.

in these two cases the MSE improves from $N = 10$ to $N = 50$, but gets slightly worse for $N = 100$. Again, this may be due to an insufficient training of the ANNs for high values of N.

8 Conclusions

In the present paper, we have shown how it is possible to implement quadratic hedging approaches in a high dimensional setting. Our strategy involves the formulation of local risk minimization and mean-variance hedging by means, respectively, of BSDEs or systems of BSDEs in high dimension, that we solve by means of the deep BSDE solver of [12]. We test the proposed methodology on Heston's stochastic volatility model. For the one-dimensional setting, we validate our algorithms against known analytical approaches showing that we can reach a high level of precision. Our approach allows us to hedge contingent claims in the presence of a high number of risk factors, a setting where traditional techniques are not feasible.

There are different directions for future work. On the one side, it could be interesting to consider counterparty credit risk problems along the lines of [18], who consider only a complete market setting. Recently, the deep solver we use has been extended to the case with jumps in [31], hence a natural idea would be to investigate whether the technique we propose could be employed in a jump-diffusion setting. Since in [17] the stochastic control approach to mean-variance hedging we are using is extended to include jumps, we conjecture that such an extension is possibile.

References

[1] S. Ankirchner and G. Heyne. Cross hedging with stochastic correlation. *Finance Stochastics*, 16(1):17–43, January 2012.

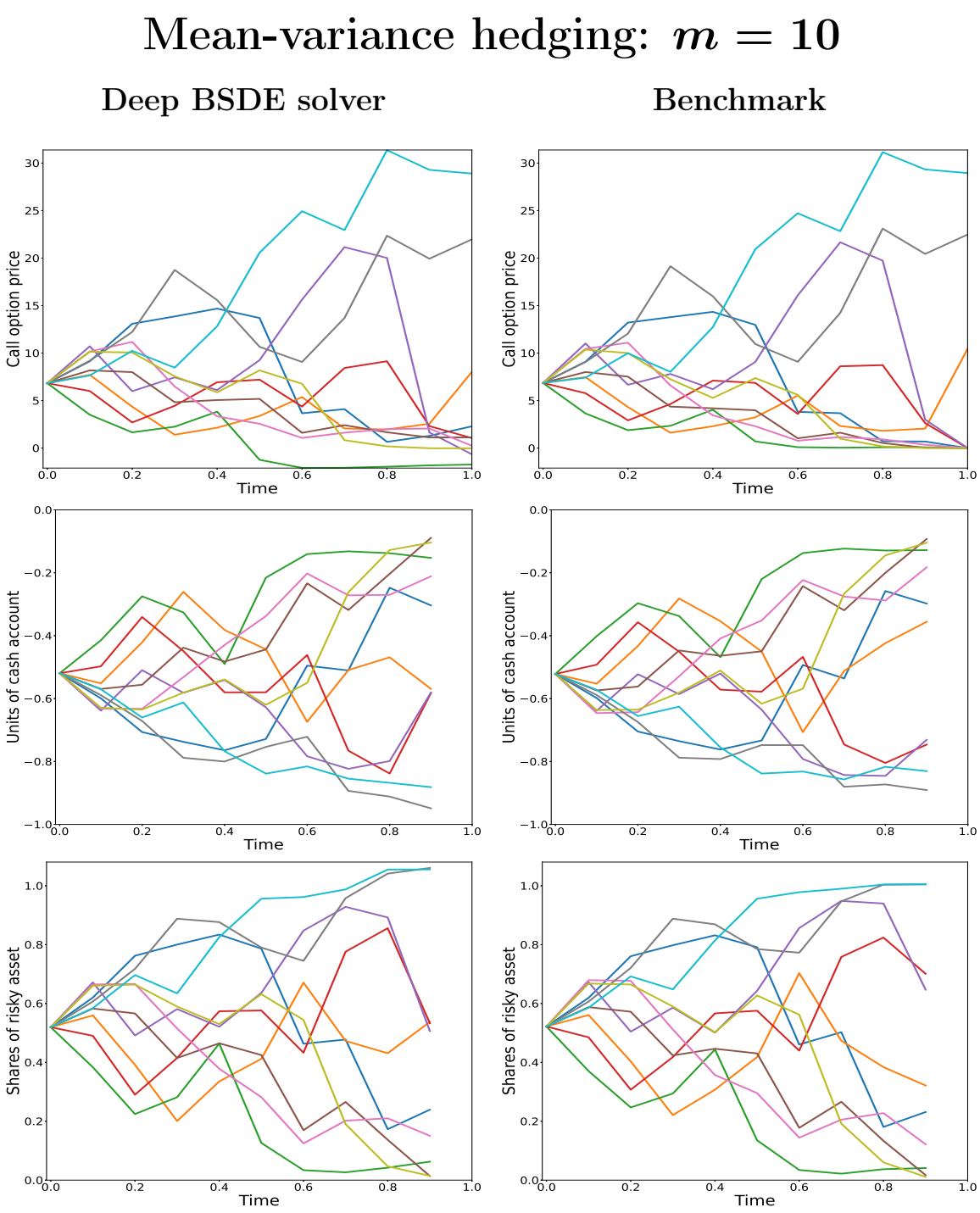

Figure 3: Deep solver solution (left) and benchmark solution (right) for the mean-variance hedging in a 10 points discretization grid for 10 random samples. From above: the call option price, the units of cash account and the shares of risky asset in the interval $[0, 1]$.

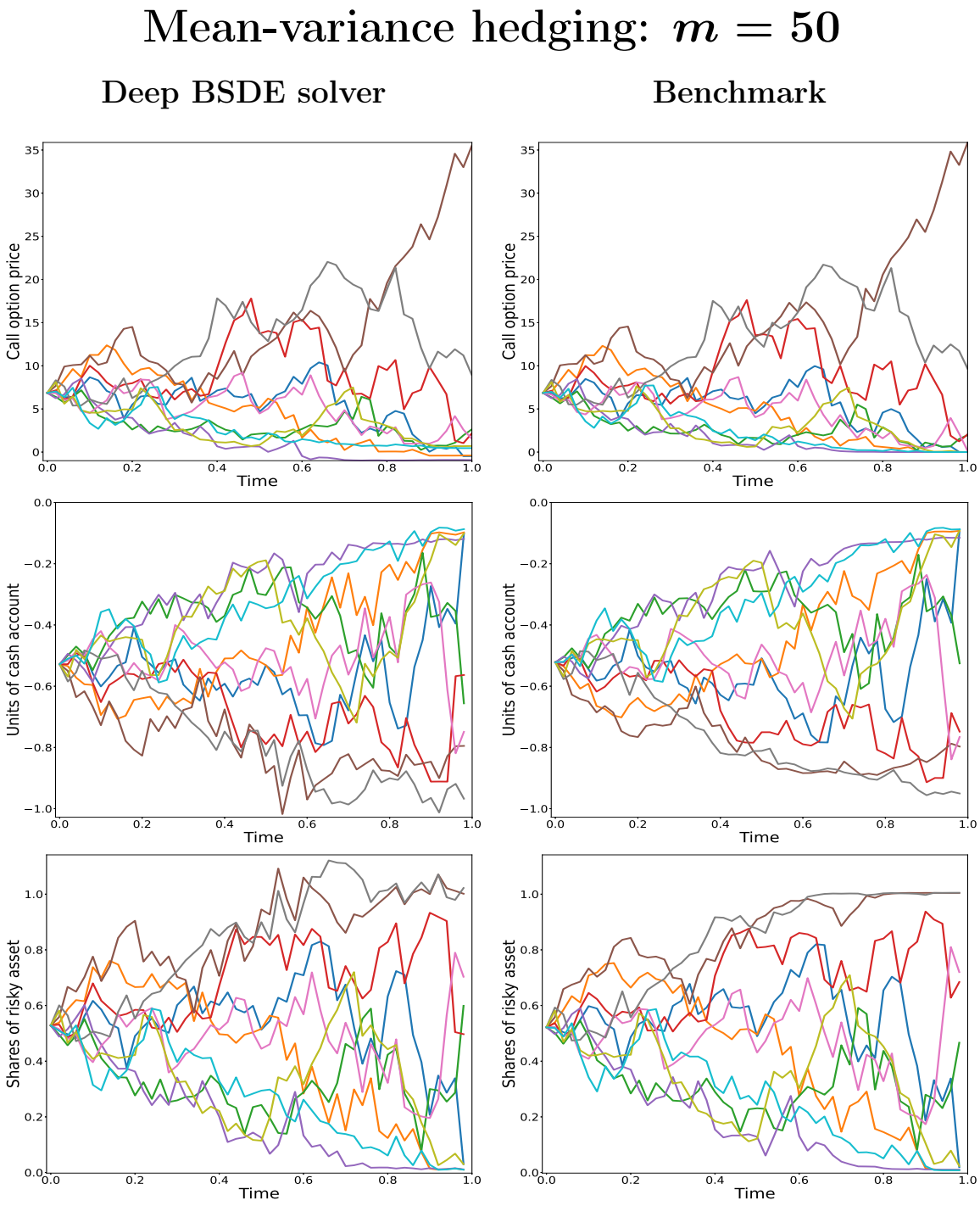

Figure 4: Deep solver solution (left) and benchmark solution (right) for the mean-variance hedging in a 50 points discretization grid for 10 random samples. From above: the call option price, the units of cash account and the shares of risky asset in the interval $[0, 1]$.

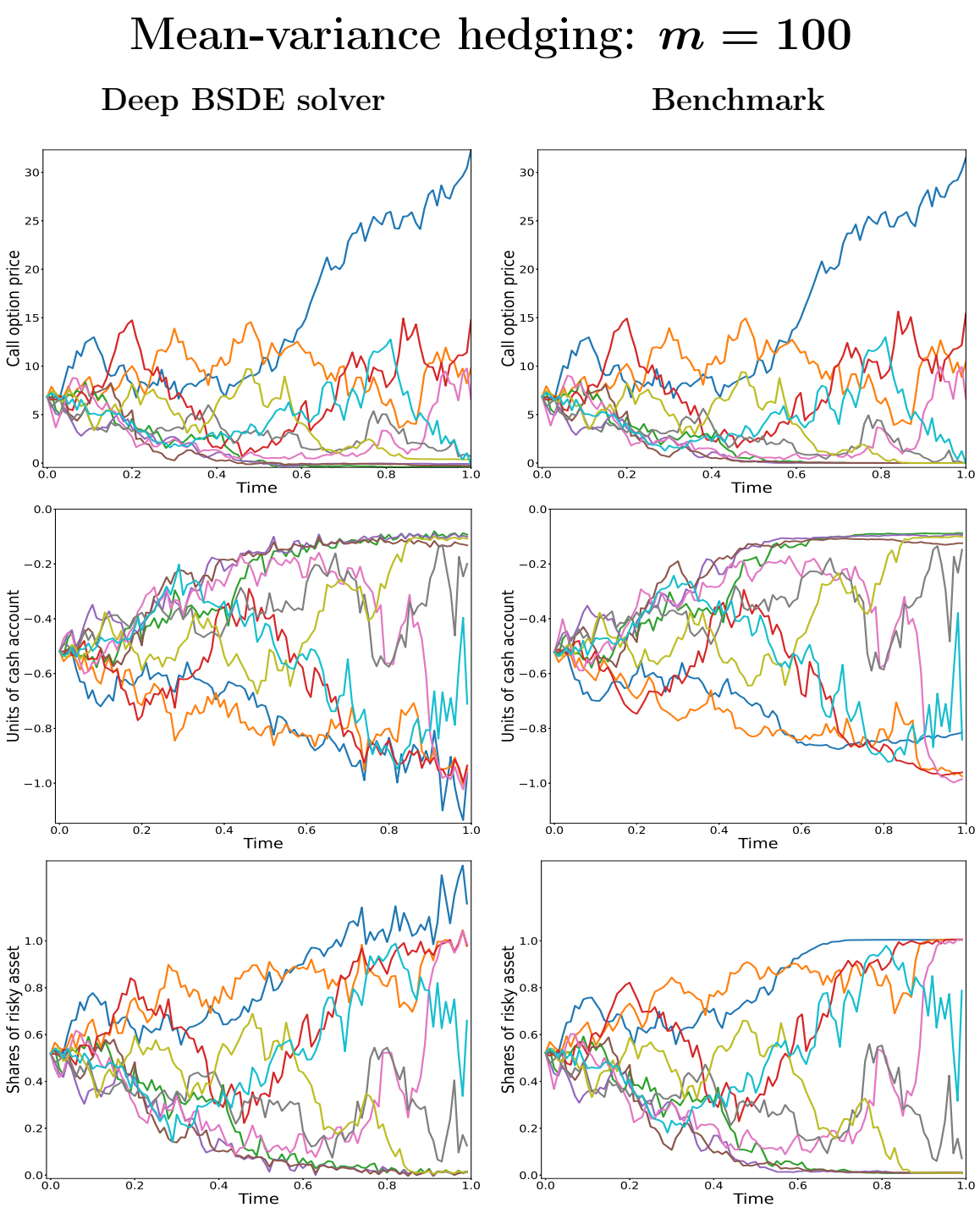

Figure 5: Deep solver solution (left) and benchmark solution (right) for the mean-variance hedging in a 100 points discretization grid for 10 random samples. From above: the call option price, the units of cash account and the shares of risky asset in the interval $[0, 1]$.

Local risk minimization

Portfolio dimension: 1			**MC price: 6.854**
Time steps	**10**	**50**	**100**
BSDE solver price	6.829	6.846	6.855
Relative error (%)	**0.360**	**0.120**	**0.0162**
Training time (s)	128	735	1546
PDE price	6.850	6.850	6.850
Relative error (%)	**0.0488**	**0.0613**	**0.0618**
Portfolio dimension: 5			**MC price: 15.412**
Time steps	**10**	**50**	**100**
BSDE solver price	15.197	15.366	15.365
Relative error (%)	**1.395**	**0.299**	**0.309**
Training time (s)	255	1250	2866
Portfolio dimension: 20			**MC price: 30.761**
Time steps	**10**	**50**	**100**
BSDE solver price	30.704	30.783	30.828
Relative error (%)	**1.322**	**0.568**	**0.218**
Training time (s)	418	1993	3660
Portfolio dimension: 100			**MC price: 68.950**
Time steps	**10**	**50**	**100**
BSDE solver price	68.269	68.427	69.020
Relative error (%)	**0.988**	**0.758**	**0.101**
Training time (s)	1772	9096	16527

Table 3: Local risk minimization results for different portfolio dimensions and different number of total time steps in the discretization grid. For each configuration, we compute the Monte Carlo (MC) price by simulating 10^5 samples under the minimal martingale measure, and we use it to compute the relative error in the classical way. For the portfolio with only one risky asset, we report the price obtained with the benchmark approach via PDE presented in Appendix A.2.

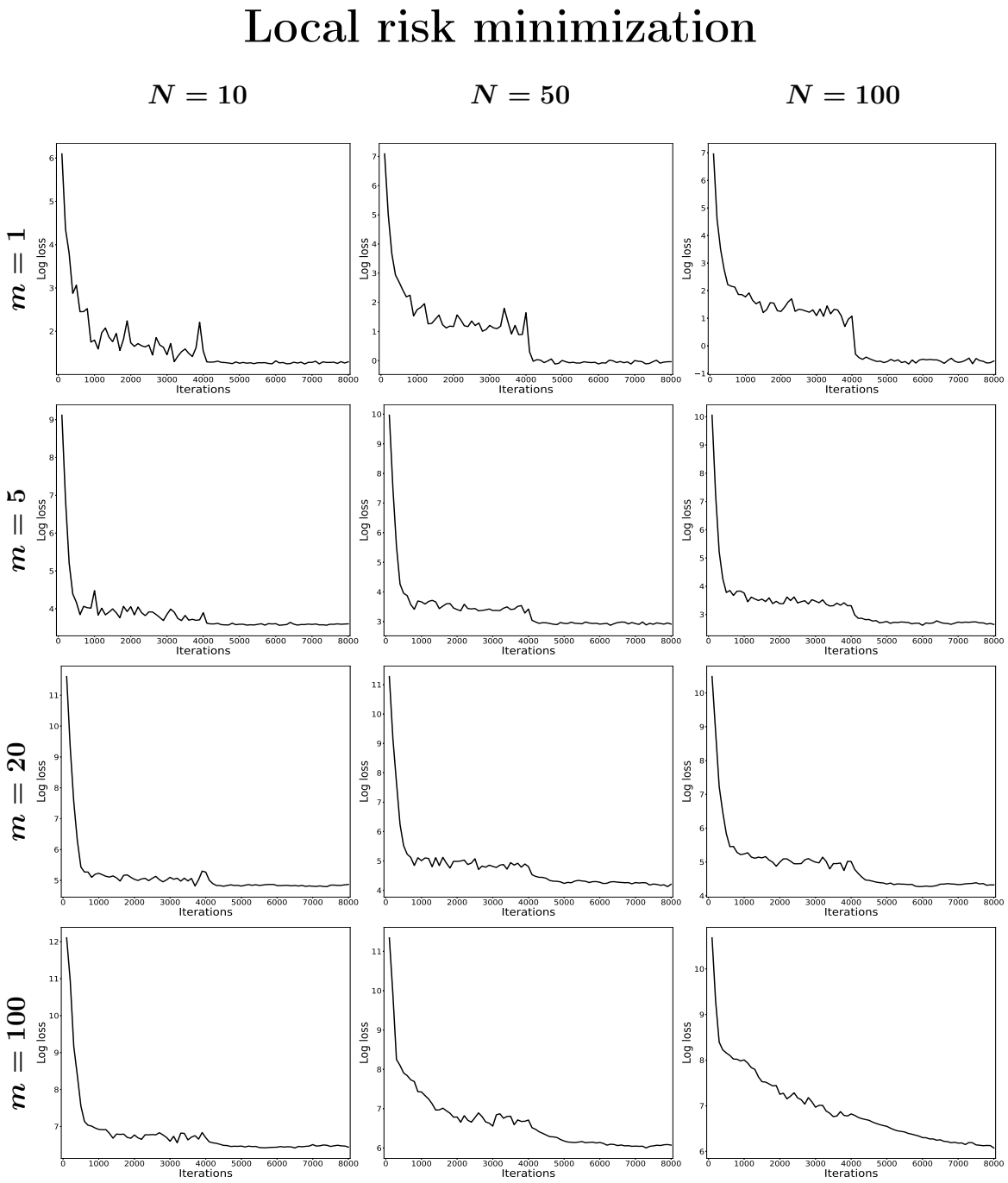

Figure 6: Logarithm of the loss functional as a function of the iteration number for the different experiment configurations presented in Table 3.

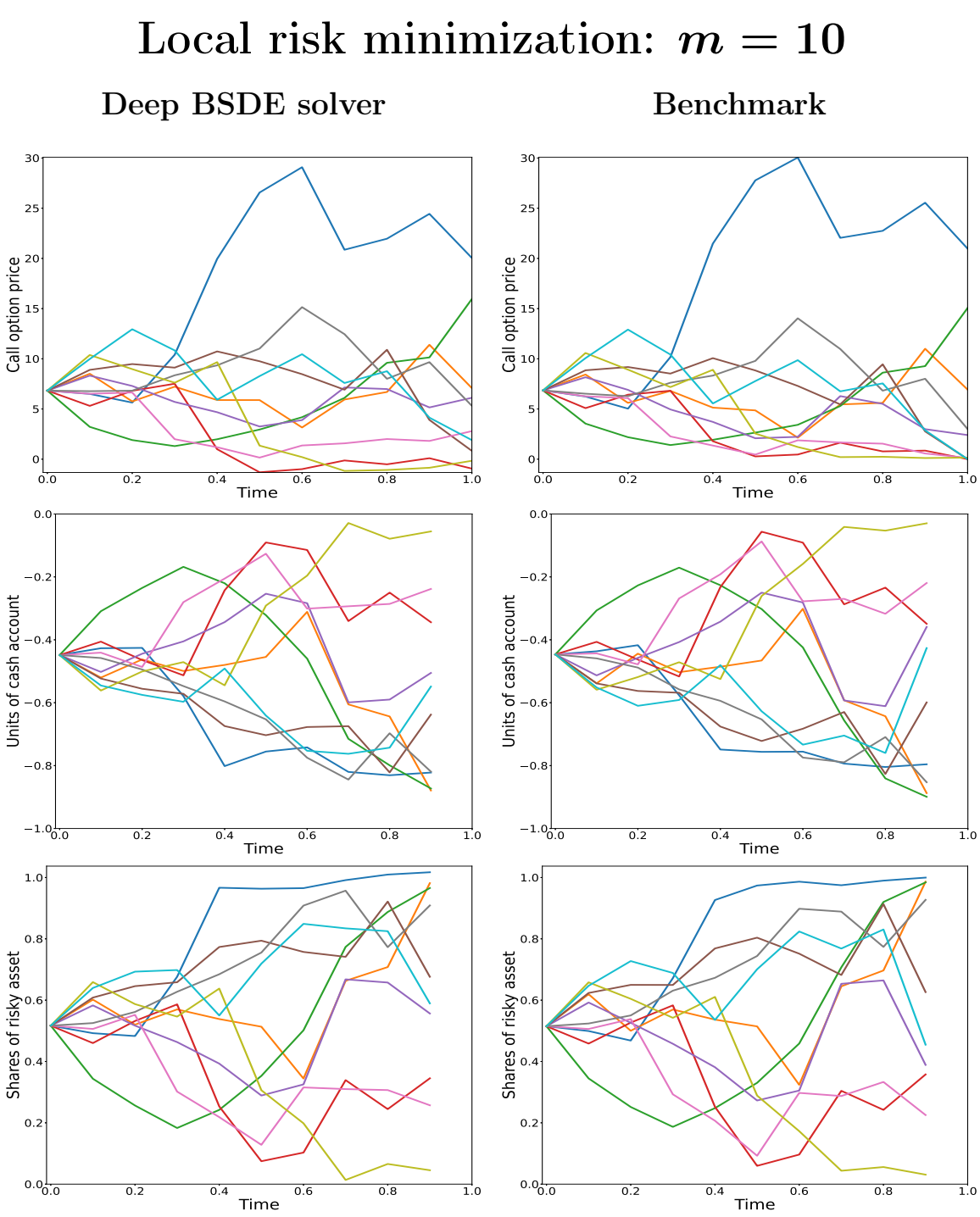

Figure 7: Deep solver solution (left) and benchmark solution (right) for the local risk minimization in a 10 points discretization grid for 10 random samples. From above: the call option price, the units of cash account and the shares of risky asset in the interval $[0, 1]$.

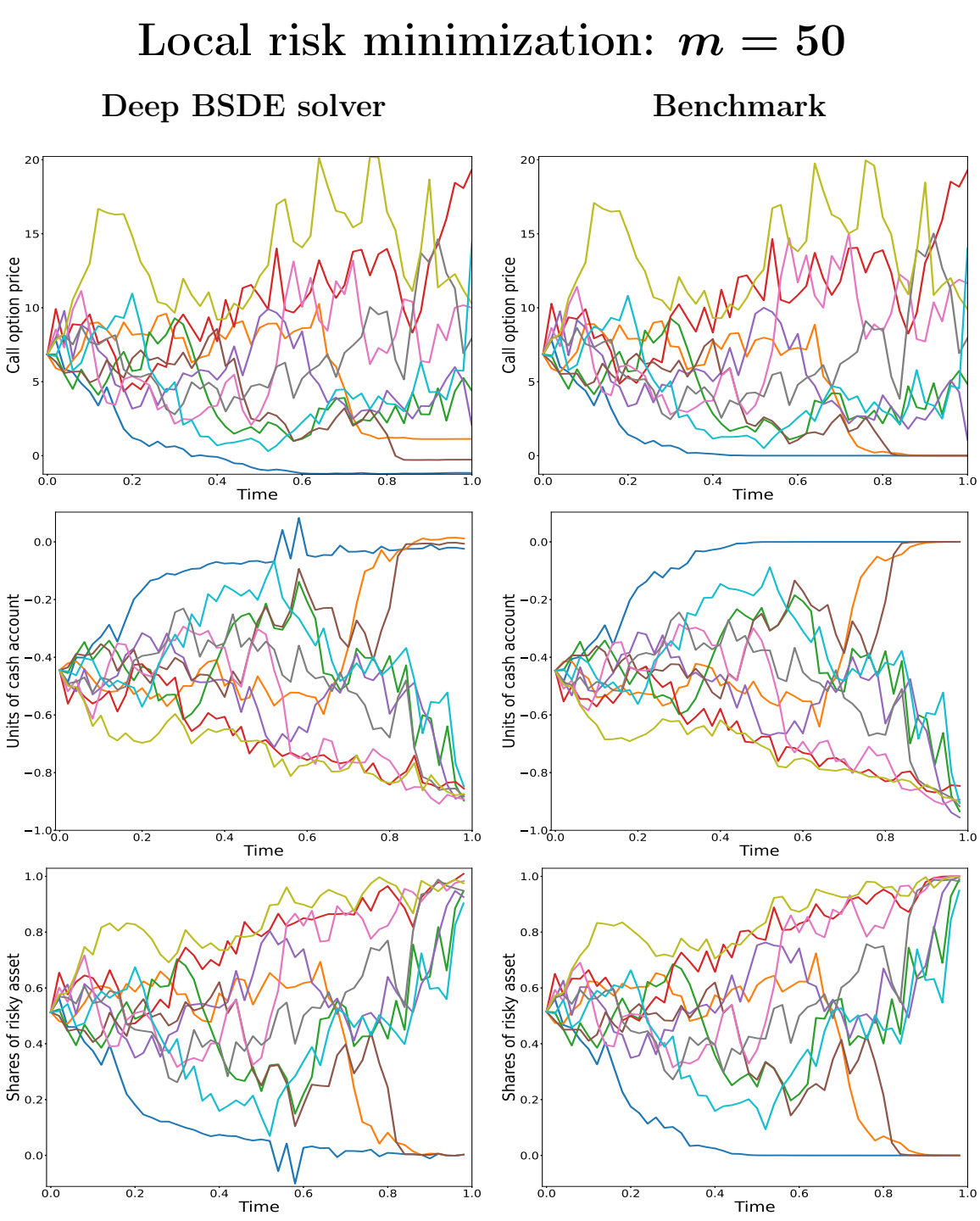

Figure 8: Deep solver solution (left) and benchmark solution (right) for the local risk minimization in a 50 points discretization grid for 10 random samples. From above: the call option price, the units of cash account and the shares of risky asset in the interval $[0, 1]$.

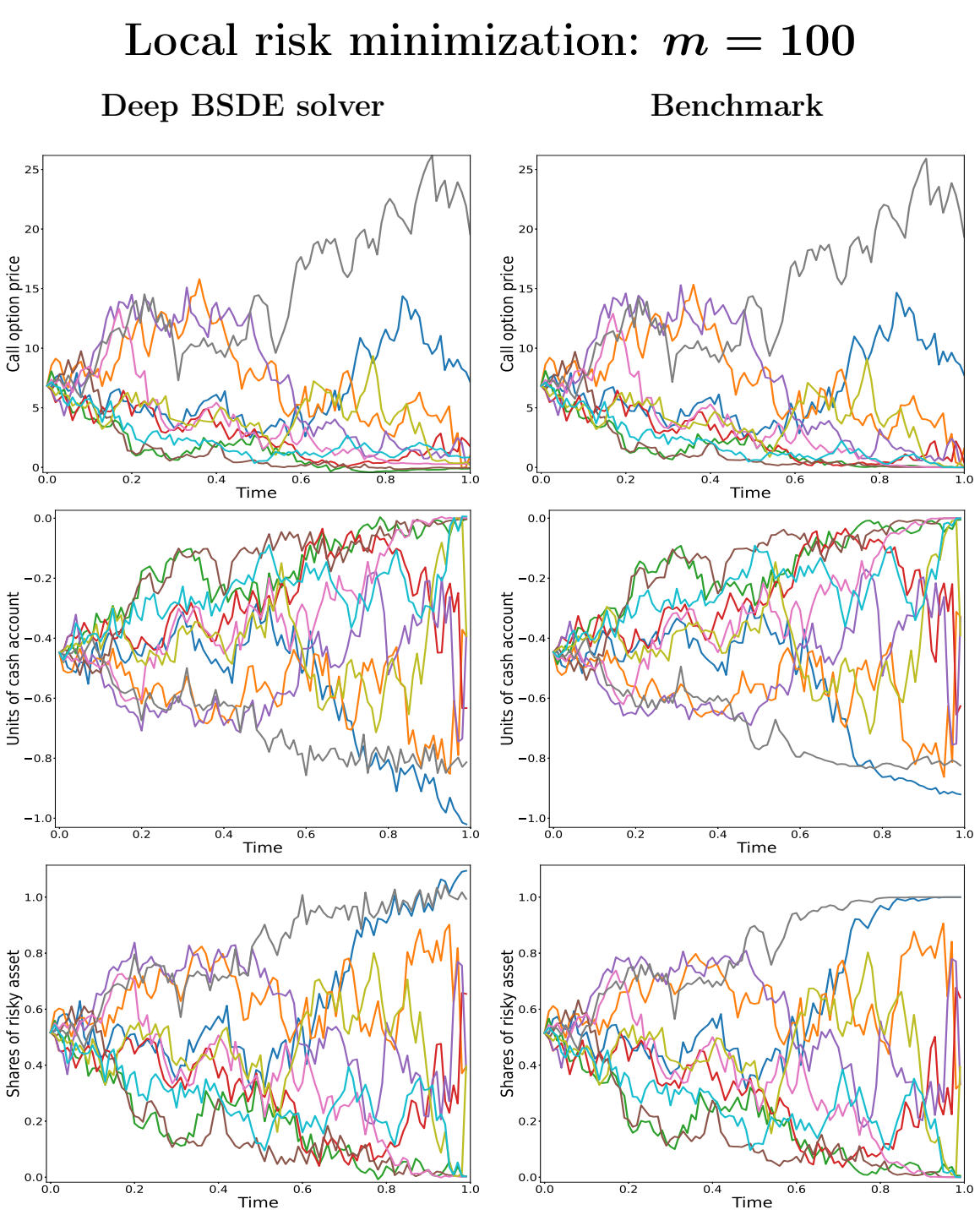

Figure 9: Deep solver solution (left) and benchmark solution (right) for the local risk minimization in a 100 points discretization grid for 10 random samples. From above: the call option price, the units of cash account and the shares of risky asset in the interval $[0, 1]$.

Mean squared error

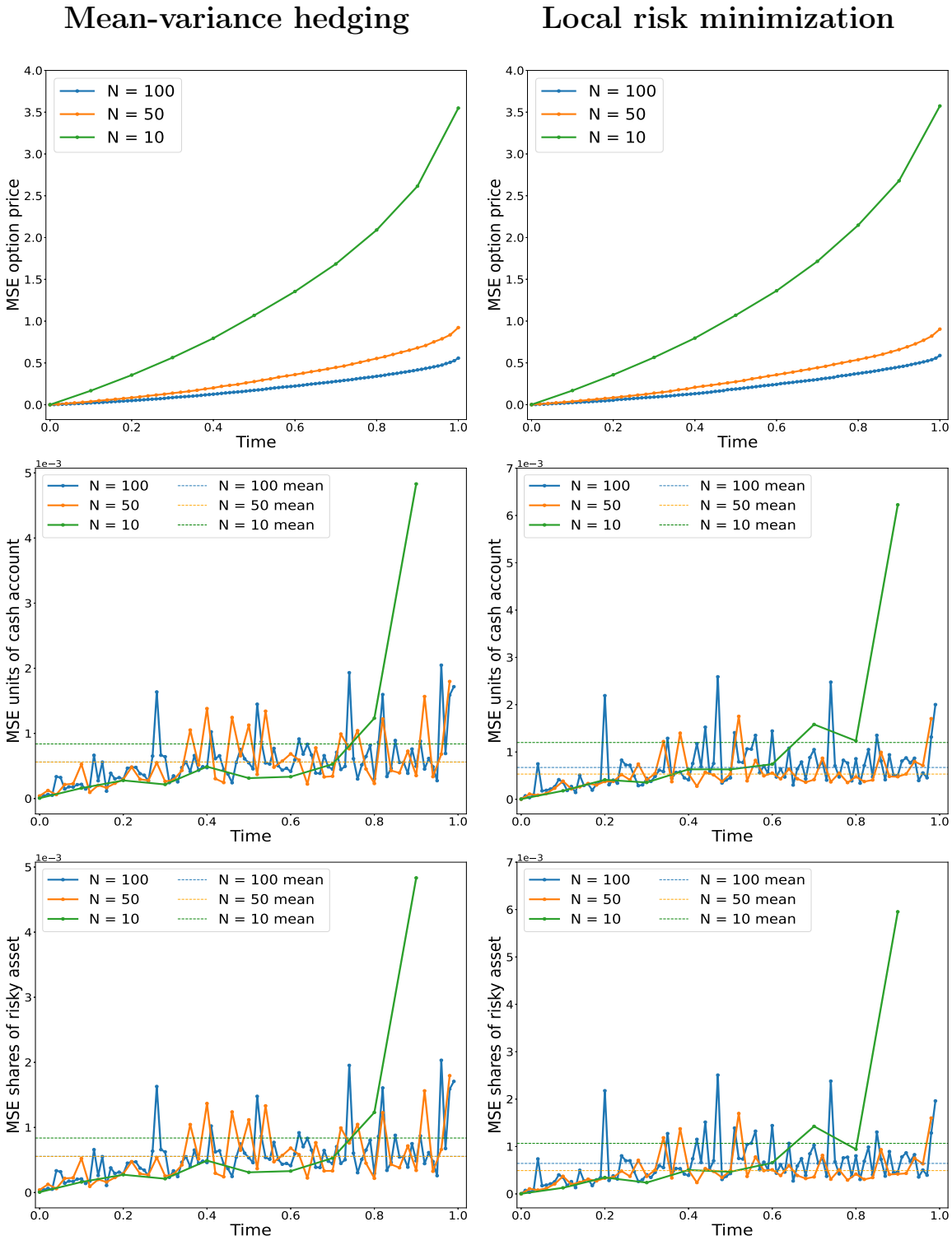

Figure 10: Mean Squared Error (MSE) for the mean-variance hedging (left) and local risk minimization (right). From above: MSE for the option price, MSE for the units of cash account and MSE for the shares of risky asset.

[2] F. Biagini, P. Guasoni, and M. Pratelli. Mean-variance hedging for stochastic volatility models. *Mathematical Finance*, 10(2):109–123, 2000.

[3] F. Black and M. Scholes. The pricing of options and corporate liabilities. *Journal of Political Economy*, 81(3):637–54, 1973.

[4] B. Bouleau and D. Lamberton. Residual risks and hedging strategies in markovian markets. *Stochastic Processes and their Applications*, 33(1):131–150, 1989.

[5] R. Carmona, editor. *Indifference Pricing*. Princeton University Press, Princeton, 2008.

[6] A. Černý and J. Kallsen. On the structure of general mean-variance hedging strategies. *The Annals of probability*, 35(4):1479–1531, 2007.

[7] A. Černý and J. Kallsen. Mean–variance hedging and optimal investment in heston's model with correlation. *Mathematical Finance*, 18(3):473–492, 2008.

[8] C. Czichowsky and Černý.

[9] L. Delong. *Backward Stochastic Differential Equations with Jumps and Their Actuarial and Financial Applications*. Springer, 2017.

[10] G. B. Di Masi, Yu. M. Kabanov, and W. J. Runggaldier. Mean-variance hedging of options on stocks with markov volatilities. *Theory of Probability & Its Applications*, 39(1):172–182, 1995.

[11] D. Duffie and H. R. Richardson. Mean-Variance Hedging in Continuous Time. *The Annals of Applied Probability*, 1(1):1 – 15, 1991.

[12] W. E, J. Han, and A. Jentzen. Deep learning-based numerical methods for high-dimensional parabolic partial differential equations and backward stochastic differential equations. *Communications in Mathematics and Statistics*, 5(4):349–380, 2017.

[13] N. El Karoui, S. Peng, and M. C. Quenez. Backward stochastic differential equations in finance. *Mathematical Finance*, 7(1):1–71, 1997.

[14] D. Filipovic. *Term-structure models*. Springer Finance Textbooks. Springer, Berlin, Germany, 2009 edition, August 2009.

[15] H. Föllmer and M. Schweizer. Hedging of contingent claims under incomplete information. In M. H. A. Davis and R. J. Elliott, editors, *Applied Stochastic Analysis*, volume 5, pages 389 – 414. Gordon and Breach, 01 1991.

[16] H. Föllmer and D. Sondermann. Hedging of non-redundant contingent claims. In W. Hildenbrand and A. Mas-Colell In Honour of G. Debreu, editors, *Contributions to Mathematical Economics*, chapter 12, pages 205–223. North-Holland, 1986.

[17] A. Gnoatto, M. Patacca, and A. Picarelli. A deep solver for BSDEs with jumps. *arXiv e-prints*, page arXiv:2211.04349, November 2022.

[18] A. Gnoatto, A. Picarelli, and C. Reisinger. Deep xVA solver - A neural network based counterparty credit risk management framework. *SIAM journal on financial mathematics - forthcoming*, 2022.

[19] J. Han, A. Jentzen, and W. E. Solving high-dimensional partial differential equations using deep learning. *Proceedings of the National Academy of Sciences*, 115(34):8505–8510, August 2018.

[20] J. Michael Harrison and Stanley R. Pliska. Martingales and stochastic integrals in the theory of continuous trading. *Stochastic Processes and their Applications*, 11(3):215–260, 1981.

[21] D. Heath, E. Platen, and M. Schweizer. A comparison of two quadratic approaches to hedging in incomplete markets. *Mathematical Finance*, 11(4):385–413, 2001.

[22] D. Heath, E. Platen, and M. Schweizer. Numerical comparison of local risk-minimisation and mean-variance hedging. In M. Musiela É. Jouini, J. Cvitanić, editor, *Option pricing, interest rates and risk management*, pages 509–537. Cambridge University Press, 2001.

[23] S. L. Heston. A closed-form solution for options with stochastic volatility with applications to bond and currency options. *The review of financial studies*, 6(2):327–343, 1993.

[24] N Hofmann, E. Platen, and M. Schweizer. Option pricing under incompleteness and stochastic volatility. *Mathematical Finance*, 2(3):153–187, 1992.

[25] KJ In't Hout and S Foulon. Adi finite difference schemes for option pricing in the heston model with correlation. *International Journal of Numerical Analysis & Modeling*, 7(2), 2010.

[26] M. Jeanblanc, M. Mania, M. Santacroce, and M. Schweizer. Mean-variance hedging via stochastic control and BSDEs for general semimartingales. *The Annals of Applied Probability*, 22(6):2388 – 2428, 2012.

[27] J. Kallsen and A. Pauwels. Variance-optimal hedging in general affine stochastic volatility models. *Advances in Applied Probability*, 42(1):83–105, 2010.

[28] M. Kobylanski. Backward stochastic differential equations and partial differential equations with quadratic growth. *The Annals of Probability*, 28(2):558 – 602, 2000.

[29] D. O. Kramkov. Optional decomposition of supermartingales and hedging contingent claims in incomplete security markets. *Probability Theory and Related Fields*, 105(4):459–479, December 1996.

[30] A. E. Lim. Quadratic hedging and mean-variance portfolio selection with random parameters in an incomplete market. *Mathematics of Operations Research*, 29(1):132–161, 2004.

[31] A. E. B. Lim. Mean-variance hedging when there are jumps. *SIAM Journal on Control and Optimization*, 44(5):1893–1922, 2005.

[32] A. Mijatović and M. Urusov. On the martingale property of certain local martingales. *Probability Theory and Related Fields*, 152(1-2):1–30, July 2010.

[33] M. Schweizer. Option hedging for semimartingales. *Stochastic Processes and their Applications*, 37(2):339–363, 1991.

[34] M. Schweizer. Approximating Random Variables by Stochastic Integrals. *The Annals of Probability*, 22(3):1536 – 1575, 1994.

[35] M. Schweizer. A guided tour through quadratic hedging approaches. In *in: É. Jouini, J. Cvitanić, M. Musiela (eds.), "Option Pricing, Interest Rates and Risk Management", Cambridge University Press*, pages 538–574. 2001.

[36] M. Schweizer. Local risk minimization for multidimensional assets and payment streams. *Banach Cent. Publ*, 83:213–229, 2008.

[37] Y. Shen and Y. Zeng. Optimal investment–reinsurance strategy for mean–variance insurers with square-root factor process. *Insurance: Mathematics and Economics*, 62:118–137, 2015.

A Semi-explicit solutions for mean-variance hedging and local risk minimization for the Heston model in one dimension

In order to compare the results of the deep BSDE solver, we derive semi-explicit solutions for the mean-variance hedging and for the local risk minimization, by adapting, respectively, the results from [7] and [22]. These will allow us to benchmark the price process and the trading strategy trajectories for the Heston model in dimension 1, see Section 7.

A.1 The mean-variance hedging of Černý and Kallsen [7]

In the mean-variance hedging, we solve recursively two BSDEs, respectively equation (3.2) and equation (3.3), and we find (an approximation of) the two processes L and $\tilde{X}^{\mathrm{mv}}$.

The process L corresponds to what Černý and Kallsen define as the *opportunity process*, which defines the so-called *opportunity-neutral measure* $\mathbb{P}^*$. This is a non-martingale equivalent measure such that variance optimal martingale measure $\mathbb{Q}_{\nu^{\mathrm{mv}}}$ introduced in Section 3 can be computed as the minimal martingale measure under $\mathbb{P}^*$, see [6] or [7] for details.

Following the approach of [7], the opportunity process is of the form

$$L^{\mathrm{CK}} = \exp\left(\chi_0 + \chi_1 Y^2\right), \tag{A.1}$$

Y^2 being the variance process for the one-dimensional Heston model (6.4), while the functions χ_0 and χ_1 are solutions of a system of Riccati ODEs, see [7, Proposition 3.2]. In particular, by adapting [7, Lemma 6.1], the functions χ_0 and χ_1 at time $t \in [0,T]$ are

$$\chi_0(t) = \mathfrak{F}\left(-\frac{\mathfrak{B}}{2\mathfrak{C}}(T-t) - \frac{1}{\mathfrak{C}}\log\left(\frac{(\mathfrak{B}+\mathfrak{D})e^{-\mathfrak{D}(T-t)/2} - (\mathfrak{B}-\mathfrak{D})e^{\mathfrak{D}(T-t)/2}}{2\mathfrak{D}}\right)\right), \tag{A.2}$$

$$\chi_1(t) = -\frac{\mathfrak{B}}{2\mathfrak{C}} + \frac{\mathfrak{D}}{2\mathfrak{C}}\frac{(\mathfrak{B}+\mathfrak{D})e^{-\mathfrak{D}(T-t)/2} + (\mathfrak{B}-\mathfrak{D})e^{\mathfrak{D}(T-t)/2}}{(\mathfrak{B}+\mathfrak{D})e^{-\mathfrak{D}(T-t)/2} - (\mathfrak{B}-\mathfrak{D})e^{\mathfrak{D}(T-t)/2}}, \tag{A.3}$$

where

$$\begin{aligned} &\mathfrak{A} := -\mu^2, && \mathfrak{B} := -\kappa - 2\rho\sigma\mu, \quad \mathfrak{C} := \tfrac{1}{2}\sigma^2(1-2\rho^2), \\ &\mathfrak{D} := \sqrt{\mathfrak{B}^2 - 4\mathfrak{A}\mathfrak{C}}, && \mathfrak{F} := \kappa\theta, \end{aligned}$$

with $\mathfrak{C}, \mathfrak{D} \neq 0$. We refer to [7, Lemma 6.1] for the case $\mathfrak{C} = 0$ and $\mathfrak{D} = 0$.

As we mentioned above, the process L^{CK} characterizes the opportunity-neutral measure $\mathbb{P}^*$. In particular, the process

$$Z_t := \frac{L_t^{\mathrm{CK}}}{L_0^{\mathrm{CK}}}\exp\left(-\int_0^t \left(\mu + \rho\sigma\chi_1(s)\right)^2 Y_s^2 ds\right) = \mathcal{E}\left(\int_0^t \sigma\chi_1(s)Y_s\left(\rho dW_s + \sqrt{1-\rho^2}dB_s\right)\right)$$

is a bounded positive martingale, and by virtue of the Girsanov theorem

$$\begin{aligned} W_t^* &= W_t - \int_0^t \rho\sigma\chi_1(s)Y_s\mathrm{d}s \\ B_t^* &= B_t - \int_0^t \sqrt{1-\rho^2}\sigma\chi_1(s)Y_s\mathrm{d}s \end{aligned} \tag{A.4}$$

are Brownian motions under $\mathbb{P}^*$, with $\mathrm{d}\mathbb{P}^*/\mathrm{d}\mathbb{P} = Z_T$. The variance optimal martingale measure coincides then with the minimal measure relative to $\mathbb{P}^*$:

$$\frac{\mathrm{d}\mathbb{Q}_{\nu^{\mathrm{mv}}}}{\mathrm{d}\mathbb{P}^*} = \mathcal{E}\left(-\int_0^T \left(\mu + \rho\sigma\chi_1(s)\right) Y_s \mathrm{d}W_s^*\right).$$

By the Girsanov theorem

$$\begin{aligned} W_t^{\mathrm{mv}} &= W_t^* + \int_0^T \left(\mu + \rho\sigma\chi_1(s)\right) Y_s\mathrm{d}s \\ B_t^{\mathrm{mv}} &= B_t^* \end{aligned} \tag{A.5}$$

are uncorrelated Brownian motions under $\mathbb{Q}_{\nu^{\mathrm{mv}}}$. By combining equation (A.4) and (A.5) with the Heston dynamics (6.4), the dynamics of $\tilde{S}$ and Y^2 under the variance optimal martingale measure become

$$\begin{cases} \mathrm{d}\tilde{S}_t = \tilde{S}_t Y_t \mathrm{d}W_t^{\mathrm{mv}} \\ \mathrm{d}Y_t^2 = \left(\kappa\theta - \kappa_t Y_t^2\right)\mathrm{d}t + \sigma Y_t\left(\rho W_t^{\mathrm{mv}} + \sqrt{1-\rho^2}B_t^{\mathrm{mv}}\right) \end{cases}, \tag{A.6}$$

with $\kappa_t := \kappa + \rho\sigma\mu - \chi_1(t)\sigma^2(1-\rho^2)$.

Let us now focus on $\tilde{X}^{\mathrm{mv}}$. Following Černý and Kallsen, if the value of the contingent claim $\tilde{H}$ is given by $g(Y_T^2, \tilde{S}_T)$, with g bounded and continuous function, we consider a function $f \in \mathcal{C}^{1,2,2}$ such that

$$\tilde{X}_t^{\mathrm{CK}} = \mathbb{E}^{\mathbb{Q}_{\nu^{\mathrm{mv}}}}\left[\tilde{H}\middle|\mathcal{F}_t\right] = f(T-t, Y_t^2, \tilde{S}_t), \tag{A.7}$$

where $\tilde{X}^{\mathrm{CK}}$ is the mean-variance hedging contingent claim price in the Černý and Kallsen approach. From [7, Proposition 4.1], the function f is the unique classical solution of the PDE

$$\begin{cases} -f_1 + \frac{1}{2}y\left(\sigma^2 f_{22} + 2\rho\sigma s f_{23} + s^2 f_{33}\right) + \left(\kappa\theta - \left(\kappa + \rho\sigma\mu - \chi_1(t)\sigma^2(1-\rho^2)\right)y\right)f_2 = 0 \\ f(0,y,s) = g(y,s) \end{cases} \tag{A.8}$$

where $f_i := \frac{\partial f}{\partial x_i}$ and $f_{ij} := \frac{\partial^2 f}{\partial x_i \partial x_j}$, for $i,j \in \{1,2,3\}$. We point out that the PDE (A.8) has time-dependent coefficients, hence we need to adapt the classical methodology for solving the Heston PDE to this situation. We consider the approach of [25], where a finite difference method is applied in the space dimension and a splitting scheme of the Alternative Direction Implicit (ADI) type is applied in the time dimension. We refer to Appendix C for a brief presentation of the methodology, or to [25] directly for a more detailed description. We denote by $\widehat{f}^n$ the approximated value of f in $(t_n, \overline{Y}_n^2, \overline{S}_n)$ and by $\widehat{f}_i^n$ its derivatives, for $n = 1, \ldots, N$ and $i \in \{1,2,3\}$. Let $\widehat{X}_n^{\mathrm{CK}}$ be the approximated $\tilde{X}^{\mathrm{CK}}$ in $t = t_n$.

Remark A.1. By solving the PDE as described in Appendix C, for each time step n we find the values of the function f on a grid for the bounded domain $[0, \mathbb{S}] \times [0, \mathbb{Y}]$ for a certain $\mathbb{S}$ and a certain $\mathbb{Y}$. Let $m_s \geq 1$ and $m_y \geq 1$ be the number of points, respectively, in the s-

and y-direction, which we denote with s_k, $k = 1, \dots, m_s$, and y_ℓ, $\ell = 1, \dots, m_y$. We then find $\widehat{f}^{(n,\ell,k)} \approx f(t_n, y_\ell, s_k)$ as the approximation of f in (t_n, y_ℓ, s_k), for $n = 1, \dots, N$.

If we want to compare $\widehat{X}^{\mathrm{mv}}$ found with the deep BSDE solver and the corresponding $\widehat{X}^{\mathrm{CK}}$ from the Černý and Kallsen approach for a specific realization of the forward process $(\tilde{S}, Y^2)$, we then need first to interpolate $\widehat{f}^{(n,\ell,k)}$ to find the right values for comparison. Namely, given a realization $(\overline{S}_n, \overline{Y}^2_n)$, for $n = 1, \dots, N$, for each time step n we need to find where the simulated $\overline{S}_n$ and $\overline{Y}^2_n$ are located in the mesh, this means to find $k \in \{1, \dots, m_s - 1\}$ and $\ell \in \{1, \dots, m_y - 1\}$ such that $\overline{S}_n \in (s_k, s_{k+1}]$ and $\overline{Y}^2_n \in (y_\ell, y_{\ell+1}]$. We then denote with $\widehat{f}^n$ the value that we obtain with a bi-linear interpolation from $\widehat{f}^{(n,\ell,k)}$, $\widehat{f}^{(n,\ell+1,k)}$, $\widehat{f}^{(n,\ell,k+1)}$ and $\widehat{f}^{(n,\ell+1,k+1)}$. Similarly if we want to compute the derivatives $\widehat{f}^n_i$.

The approximated optimal trading strategy and the corresponding value process can then be recursively computed starting from [7, Equations (3.3) and (4.1)] as follows:

$$\begin{cases} \widehat{V}^{\mathrm{CK}}_0 = y \\ \widehat{\xi}^{\mathrm{CK}}_n = \widehat{f}^n_3 + \frac{\rho\sigma \widehat{f}^n_2}{\overline{S}_n} + \frac{\mu + \rho\sigma\chi^n_1}{\overline{S}_n} \left(\widehat{f}^n - \widehat{V}^{\mathrm{CK}}_n \right) \\ \widehat{\psi}^{\mathrm{CK}}_n = \widehat{V}^{\mathrm{CK}}_n - \widehat{\xi}^{\mathrm{CK}}_n \overline{S}_n \\ \widehat{V}^{\mathrm{CK}}_{n+1} = \widehat{V}^{\mathrm{CK}}_n + \widehat{\xi}^{\mathrm{CK}}_n \left(\overline{S}_{n+1} - \overline{S}_n \right) \end{cases} \tag{A.9}$$

where $\chi^n_1 = \chi_1(t_n)$.

A.2 The local risk minimization of Heath, Platen and Schweizer [22]

In the local risk minimization we solve the BSDE (4.7) and we find (an approximation of) the process $\tilde{X}^{\mathrm{lr}}$ by means of the deep BSDE solver. If the dimension is $d = 1$, we can alternatively follow the approach of [22].

As in the mean variance setting, we assume that the value of the contingent claim $\tilde{H}$ is given by a function $g(Y^2_T, \tilde{S}_T)$. Then, there exists a function $f \in \mathcal{C}^{1,2,2}$ such that

$$\tilde{X}^{\mathrm{HPS}}_t = \mathbb{E}^{\mathbb{Q}^{\mathrm{lr}}} \left[\tilde{H} \middle| \mathcal{F}_t \right] = f(T - t, Y^2_t, \tilde{S}_t), \tag{A.10}$$

where $\tilde{X}^{\mathrm{HPS}}$ is the local risk minimizing contingent claim price in the Heath, Platen and Schweizer approach. By adapting the results of [22, Section 2], the function f is the unique classical solution of the PDE

$$\begin{cases} -f_1 + \frac{1}{2} y \left(\sigma^2 f_{22} + 2\rho\sigma s f_{23} + s^2 f_{33} \right) + (\kappa\theta - (\kappa + \rho\sigma\mu) y) f_2 = 0 \\ f(0, y, s) = g(y, s) \end{cases} \tag{A.11}$$

where $f_i := \frac{\partial f}{\partial x_i}$ and $f_{ij} := \frac{\partial^2 f}{\partial x_i \partial x_j}$, for $i, j \in \{1, 2, 3\}$.

Once solved (A.11) with the solver described in Appendix C, we denote by $\widehat{f}^n$ the approximated value of f in $(t_n, \overline{Y}^2_n, \overline{S}_n)$ and by $\widehat{f}^n_i$ its derivatives, for $n = 1, \dots, N$ and $i \in \{1, 2, 3\}$. Of course, the same arguments of Remark A.1 apply here. The approximated optimal trading strategy can then be computed from [22, Equation (2.3)]:

$$\begin{cases} \widehat{\xi}^{\mathrm{HPS}}_n = \widehat{f}^n_3 + \frac{\rho\sigma \widehat{f}^n_2}{\overline{S}_n}, \\ \widehat{\psi}^{\mathrm{HPS}}_n = \widehat{f}^n - \overline{S}_n \widehat{\xi}^{\mathrm{HPS}}_n, \end{cases} \quad \text{for } n = 0, \dots, N - 1. \tag{A.12}$$

B Proof of Proposition 3.1

To ease notations, we omit the superscript $^{\text{mv}}$ in the computations below. Since we work with discounted quantities, for the sake of clarity we adapt the steps of [30], Proposition 3.3. The dynamics of the discounted wealth satisfy

$$\mathrm{d}\widetilde{V}_t = \xi_t^\top \operatorname{diag}(\tilde{S}_t)\left(\mu_t - r_t\mathbb{1}\right)\mathrm{d}t + \xi_t^\top \operatorname{diag}(\widetilde{S}_t)\sigma_t \mathrm{d}W_t.$$

We also have

$$\mathrm{d}\widetilde{X}_t = \frac{1}{S_t^0}\left(\left(\phi_t^\top \eta_{1,t} - \frac{\Lambda_{2,t}^\top \eta_{2,t}}{L_t}\right)\mathrm{d}t + \eta_{1,t}^\top \mathrm{d}W_t + \eta_{2,t}^\top \mathrm{d}B_t\right),$$

hence

$$\begin{aligned}\mathrm{d}(\widetilde{X} - \widetilde{V})_t = &\left(\frac{1}{S_t^0}\left(\phi_t^\top \eta_{1,t} - \frac{\Lambda_{2,t}^\top \eta_{2,t}}{L_t}\right) - \xi_t^\top \operatorname{diag}(\tilde{S}_t)\left(\mu_t - r_t\mathbb{1}\right)\right)\mathrm{d}t \\ &+ \left(\frac{1}{S_t^0}\eta_{1,t}^\top - \xi_t^\top \operatorname{diag}(\tilde{S}_t)\sigma_t\right)\mathrm{d}W_t + \frac{1}{S_t^0}\eta_{2,t}^\top \mathrm{d}B_t.\end{aligned}$$

Now,

$$\mathrm{d}\left(\widetilde{X} - \widetilde{V}\right)_t^2 = 2\left(\widetilde{X}_t - \widetilde{V}_t\right)\mathrm{d}(\widetilde{X} - \widetilde{V})_t + \mathrm{d}\langle \widetilde{X} - \widetilde{V}\rangle_t$$

where

$$\begin{aligned}\mathrm{d}\langle \widetilde{X} - \widetilde{V}\rangle_t = \Bigg(&\frac{1}{\left(S_t^0\right)^2}\eta_{1,t}^\top \eta_{1,t} + \left(\xi_t^\top \operatorname{diag}(\tilde{S}_t)\sigma_t\right)\left(\xi_t^\top \operatorname{diag}(\tilde{S}_t)\sigma_t\right)^\top \\ &-2\frac{1}{S_t^0}\eta_{1,t}^\top\left(\xi_t^\top \operatorname{diag}(\tilde{S}_t)\sigma_t\right) + \frac{1}{\left(S_t^0\right)^2}\eta_{2,t}^\top \eta_{2,t}\Bigg)\mathrm{d}t.\end{aligned}$$

Regrouping terms

$$\begin{aligned}\mathrm{d}\left(\widetilde{X} - \widetilde{V}\right)_t^2 = &\left[2\left(\widetilde{X}_t - \widetilde{V}_t\right)\left[\frac{1}{S_t^0}\phi_t^\top \eta_{1,t} - \frac{\Lambda_{2,t}^\top \eta_{2,t}}{L_t}\right] + \frac{1}{\left(S_t^0\right)^2}\eta_{1,t}^\top \eta_{1,t} + \frac{1}{\left(S_t^0\right)^2}\eta_{2,t}^\top \eta_{2,t}\right. \\ &+ \xi_t^\top \operatorname{diag}(\tilde{S}_t)\sigma_t\sigma_t^\top \operatorname{diag}(\tilde{S}_t)\xi_t \\ &- 2\xi_t^\top \operatorname{diag}(\tilde{S}_t)\left[\left(\mu_t - r_t\mathbb{1}\right)\left(\widetilde{X}_t - \widetilde{V}_t\right) + \sigma_t\frac{\eta_{1,t}}{S_t^0}\right]dt \\ &+ 2\left(\widetilde{X}_t - \widetilde{V}_t\right)\left(\frac{1}{S_t^0}\eta_{1,t}^\top - \xi_t^\top \operatorname{diag}(\tilde{S}_t)\sigma_t\right)\mathrm{d}W_t + 2\left(\tilde{X}_t - \widetilde{V}_t\right)\frac{1}{S_t^0}\eta_{2,t}^\top \mathrm{d}B_t.\end{aligned}$$

We apply again the Itô formula

$$\mathrm{d}L_t\left(\widetilde{X}_t - \widetilde{V}_t\right)^2 = \left(\widetilde{X}_t - \widetilde{V}_t\right)^2 \mathrm{d}L_t + L_t\mathrm{d}(\widetilde{X} - \widetilde{V})_t^2 + \mathrm{d}\left\langle L, \left(\widetilde{X} - \widetilde{V}\right)\right\rangle_t.$$

The covariation term is given by

$$\mathrm{d}\left\langle L, \left(\widetilde{X}-\widetilde{V}\right)\right\rangle_t = 2\left(\widetilde{X}_t-\widetilde{V}_t\right)\left(\frac{1}{S_t^0}\eta_{1,t}^\top - \xi_t^\top \operatorname{diag}(\widetilde{S}_t)\sigma_t\right)\Lambda_{1,t} + 2\left(\widetilde{X}_t-\widetilde{V}_t\right)\frac{1}{S_t^0}\eta_{2,t}^\top\Lambda_{2,t}\mathrm{d}t,$$

hence

$$\begin{aligned}
\mathrm{d}L_t\left(\widetilde{X}_t-\widetilde{V}_t\right)^2 &= \left(\widetilde{X}_t-\widetilde{V}_t\right)^2\left[\left(|\phi_t|^2 L_t + 2\phi_t^\top\Lambda_{1,t} + \frac{\Lambda_{1,t}^\top\Lambda_{1,t}}{L_t}\right)\mathrm{d}t + \Lambda_{1,t}^\top \mathrm{d}W_t + \Lambda_{2,t}^\top \mathrm{d}B_t\right] \\
&\quad + L_t\left\{\left[2\left(\widetilde{X}_t-\widetilde{V}_t\right)\left[\frac{1}{S_t^0}\phi_t^\top\eta_{1,t} - \frac{\Lambda_{2,t}^\top\eta_{2,t}}{L_t}\right] + \frac{1}{\left(S_t^0\right)^2}\eta_{1,t}^\top\eta_{1,t} + \frac{1}{\left(S_t^0\right)^2}\eta_{2,t}^\top\eta_{2,t}\right.\right. \\
&\quad + \xi_t^\top \operatorname{diag}(\tilde{S}_t)\sigma_t\sigma_t^\top\operatorname{diag}(\tilde{S}_t)\xi_t \\
&\quad - 2\xi_t^\top\operatorname{diag}(\tilde{S}_t)\left[(\mu_t - r_t\mathbb{1})\left(\widetilde{X}_t-\widetilde{V}_t\right) + \sigma_t\frac{\eta_{1,t}}{S_t^0}\right]dt \\
&\quad \left.\left. + 2\left(\widetilde{X}_t-\widetilde{V}_t\right)\left(\frac{1}{S_t^0}\eta_{1,t}^\top - \xi_t^\top\operatorname{diag}(\tilde{S}_t)\sigma_t\right)\mathrm{d}W_t + 2\left(\tilde{X}_t-\widetilde{V}_t\right)\frac{1}{S_t^0}\eta_{2,t}^\top\mathrm{d}B_t\right\}\right. \\
&\quad + 2\left(\widetilde{X}_t-\widetilde{V}_t\right)\left(\frac{1}{S_t^0}\eta_{1,t}^\top - \xi_t^\top\operatorname{diag}(\widetilde{S}_t)\sigma_t\right)\Lambda_{1,t} + 2\left(\widetilde{X}_t-\widetilde{V}_t\right)\frac{1}{S_t^0}\eta_{2,t}^\top\Lambda_{2,t}\mathrm{d}t.
\end{aligned}$$

Some lengthy computations show that the drift term can be expressed in the following form:

$$\begin{aligned}
\mathrm{d}L_t\left(\widetilde{X}_t-\widetilde{V}_t\right)^2 &= \left\{L_t\left[\operatorname{diag}\left(\tilde{S}_t\right)\xi_t - \left(\sigma_t\sigma_t^\top\right)^{-1}\left(\left[(\mu_t - r_t\mathbb{1})^\top + \frac{\sigma_t\Lambda_{1,t}}{L_t}\right]\left(\widetilde{X}_t-\widetilde{V}_t\right) + \sigma_t\frac{\eta_{1,t}}{S_t^0}\right)\right]^\top\right. \\
&\quad \times \sigma_t\sigma_t^\top\left[\operatorname{diag}\left(\tilde{S}_t\right)\xi_t - \left(\sigma_t\sigma_t^\top\right)^{-1}\left(\left[(\mu_t - r_t\mathbb{1})^\top + \frac{\sigma_t\Lambda_{1,t}}{L_t}\right]\left(\widetilde{X}_t-\widetilde{V}_t\right) + \sigma_t\frac{\eta_{1,t}}{S_t^0}\right)\right] \\
&\quad \left. + \frac{L_t}{\left(S_t^0\right)^2}\eta_{2,t}^\top\eta_{2,t}\right\}\mathrm{d}t \\
&\quad + \left(2\left(\widetilde{X}_t-\widetilde{V}_t\right)\left(\frac{1}{S_t^0}\eta_{1,t}^\top - \xi_t^\top\operatorname{diag}(\tilde{S}_t)\sigma_t\right) + \left(\widetilde{X}_t-\widetilde{V}_t\right)^2\Lambda_{1,t}^\top\right)\mathrm{d}W_t \\
&\quad + \left(2\left(\tilde{X}_t-\widetilde{V}_t\right)\frac{1}{S_t^0}\eta_{2,t}^\top + \left(\widetilde{X}_t-\widetilde{V}_t\right)^2\Lambda_{2,t}^\top\right)\mathrm{d}B_t.
\end{aligned}$$

Let us introduce a localizing sequence $(\tau_k)_{k\in\mathbb{N}}$ with $\tau_k \nearrow \infty$ as $k\to\infty$. We fix $t\in[0,T]$, integrate on both sides and take expectations

$$\begin{aligned}
\mathbb{E}\left[L_{t\wedge\tau_k}\left(\widetilde{X}_{t\wedge\tau_k}-\widetilde{V}_{t\wedge\tau_k}\right)^2\right] &= L_0\left(\widetilde{X}_0-\widetilde{V}_0\right)^2 \\
&\quad + \mathbb{E}\left[\int_0^{t\wedge\tau_k}\left\{L_s\left[\operatorname{diag}\left(\tilde{S}_s\right)\xi_s - \left(\sigma_s\sigma_s^\top\right)^{-1}\left(\left[(\mu_s - r_s\mathbb{1})^\top + \frac{\sigma_s\Lambda_{1,s}}{L_s}\right]\left(\widetilde{X}_s-\widetilde{V}_s\right) + \sigma_s\frac{\eta_{1,s}}{S_s^0}\right)\right]^\top\right.\right. \\
&\qquad \times \sigma_s\sigma_s^\top\left[\operatorname{diag}\left(\tilde{S}_s\right)\xi_s - \left(\sigma_s\sigma_s^\top\right)^{-1}\left(\left[(\mu_s - r_s\mathbb{1})^\top + \frac{\sigma_s\Lambda_{1,s}}{L_s}\right]\left(\widetilde{X}_s-\widetilde{V}_s\right) + \sigma_s\frac{\eta_{1,s}}{S_s^0}\right)\right] \\
&\qquad \left.\left. + \frac{L_s}{\left(S_s^0\right)^2}\eta_{2,s}^\top\eta_{2,s}\right\}\mathrm{d}s\right].
\end{aligned} \tag{B.1}$$

We let $k \to \infty$ and set $t = T$. The right-hand side converges by monotone convergence. From to the definition of admissibility that we currently assume, the left-hand side converges to $\mathbb{E}\left[\left(\widetilde{X}_T - \widetilde{V}_T\right)^2\right]$ since we also have $L_T = 1$. The expression is minimized by choosing

$$\xi_t^\star = \operatorname{diag}\left(\tilde{S}_t\right)^{-1}\left(\sigma_t\sigma_t^\top\right)^{-1}\left(\left[\left(\mu_t - r_t\mathbb{1}\right)^\top + \frac{\sigma_t\Lambda_{1,t}}{L_t}\right]\left(\widetilde{X}_t - \widetilde{V}_t\right) + \sigma_t\frac{\eta_{1,t}}{S_t^0}\right).$$

It remains to show that $\xi^\star$ is admissible. For this aim, we substitute $\xi^\star$ into (B.1) and we obtain

$$\mathbb{E}\left[L_{t\wedge\tau_k}\left(\widetilde{X}_{t\wedge\tau_k} - \widetilde{V}_{t\wedge\tau_k}\right)^2\right] = L_0\left(\widetilde{X}_0 - \widetilde{V}_0\right)^2 + \mathbb{E}\left[\int_0^{t\wedge\tau_k}\frac{L_s}{\left(S_s^0\right)^2}\eta_{2,s}^\top\eta_{2,s}\mathrm{d}s\right].$$

We know that L is bounded in $(0,1]$. Also, since the interest rate r is bounded, so is the denominator $\left(S_\cdot^0\right)^2$. We also know that $\eta_2 \in L^2_{\mathbb{F}}([0,T];\mathbb{R}^m)$, hence, for any choice of t and k we have

$$\mathbb{E}\left[\int_0^{t\wedge\tau_k}\frac{L_s}{\left(S_s^0\right)^2}\eta_{2,s}^\top\eta_{2,s}\mathrm{d}s\right] \le \mathcal{C}\mathbb{E}\left[\int_0^T\eta_{2,s}^\top\eta_{2,s}\mathrm{d}s\right] < \infty,\ \mathcal{C}\in\mathbb{R}_+,$$

hence the quantity $L_{t\wedge\tau_k}\left(\widetilde{X}_{t\wedge\tau_k} - \widetilde{V}_{t\wedge\tau_k}\right)^2$ is uniformly integrable for any localizing sequence $(\tau_k)_{k\in\mathbb{N}}$, hence $\xi^\star$ is admissible.

C The Heston-PDE solver

We briefly present in this section the numerical scheme that we use for solving the two Heston PDEs arising, respectively, in the mean-variance hedging, Section A.1, and in the local risk hedging, Section A.2, for the one-dimensional case. The idea is to first discretize in the spatial variables, and then to apply a splitting scheme of the Alternating Direction Implicit (ADI) type. In particular, we follow the approach proposed by [25], with the only difference that we allow the coefficient of the derivative w.r.t. the price to depend on time. Since the rest of the algorithm is unchanged, we shall omit details such as the meshes and the finite difference schemes applied. These can be found in [25].

Let $f(T-t,y,s)$ denote the price of a European-type option with maturity T and payoff function $g:\mathbb{R}_+\times\mathbb{R}_+\to\mathbb{R}_+$, whose underlying has price at time t equal to s and volatility equal to y. Under the Heston model (6.4), the price f satisfies the parabolic PDE

$$\begin{cases} -f_1 + \frac{1}{2}y\left(\sigma^2 f_{22} + 2\rho\sigma s f_{23} + s^2 f_{33}\right) + \kappa_t\left(\theta_t - y\right)f_2 = 0, \\ f(0,y,s) = g(y,s) \\ f(t,y,0) = 0, \qquad \text{for } 0\le t\le T, \end{cases} \tag{C.1}$$

where $f_i := \frac{\partial f}{\partial x_i}$ and $f_{ij} := \frac{\partial^2 f}{\partial x_i\partial x_j}$, with $i,j\in\{1,2,3\}$. Here $\kappa:\mathbb{R}_+\to\mathbb{R}_+$ and $\theta:\mathbb{R}_+\to\mathbb{R}_+$. We point out that equation (C.1) reduces to the classical Heston PDE when $\kappa_t\equiv\kappa$ and $\theta_t\equiv\theta$ for every $0\le t\le T$, with κ and θ as in equation (6.4). Moreover, for the mean-variance hedging in Section A.1 one has that

$$\begin{cases} \kappa_t = \kappa + \rho\sigma\mu - \chi_1(t)\sigma^2(1-\rho^2), \\ \theta_t = \frac{\kappa\theta}{\kappa_t}, \end{cases} \tag{C.2}$$

and for the local risk hedging in Section A.2 one has that

$$\begin{cases} \kappa_t = \kappa + \rho\sigma\mu, \\ \theta_t = \frac{\kappa\theta}{\kappa_t}. \end{cases} \tag{C.3}$$

For numerical purposes, we restrict the spatial domain to a bounded set $[0, \mathbb{S}] \times [0, \mathbb{Y}]$. In particular, we shall consider $\mathbb{S} = 8K$ and $\mathbb{Y} = 5$. This is followed by two additional conditions at $s = \mathbb{S}$ and at $y = \mathbb{Y}$:

$$f_3(t, y, \mathbb{S}) = 1 \quad \text{and} \quad f(t, \mathbb{Y}, s) = s, \qquad \text{for } 0 \le t \le T. \tag{C.4}$$

We then apply non-uniform meshes in both the s- and y-direction, so that relatively many mesh points lie in the neighborhood of $s = K$ and $y = 0$, respectively (see [25, Section 2.2] for details). We denote with $m_s \ge 1$ and $m_y \ge 1$ the number of points, respectively, in the s- and y-direction.

The finite difference discretization yields an initial value problem for a large system of ordinary differential equation of the form

$$\begin{cases} F_t' = A_t F_t + b_t, \qquad \text{for } 0 \le t \le T, \\ F_0 = f_0. \end{cases} \tag{C.5}$$

Here $A_t \in \mathbb{R}^{\mathfrak{m}\times\mathfrak{m}}$, $b_t \in \mathbb{R}^{\mathfrak{m}}$ and $f_0 \in \mathbb{R}^{\mathfrak{m}}$, for $\mathfrak{m} := m_s m_y$. In particular, f_0 is obtained from the initial condition in (C.1) and the vector function b_t depends on the boundary conditions in (C.1) and (C.4). We solve (C.5) by applying the modified Craig-Sneyd scheme as described in [25, Section 2.3], which we adapt so to allow the time-dependent coefficients κ and θ.